Large-N approach to the two-channel Kondo lattice

Ari Wugalter, Yashar Komijani, and Piers Coleman

Phys. Rev. B **101**, 075133 — Published 24 February 2020

DOI: 10.1103/PhysRevB.101.075133

Large-N Approach to the Two-Channel Kondo Lattice

Ari Wugalter,[1] Yashar Komijani,[1] and Piers Coleman[1,2]

[1] *Center for Materials Theory, Rutgers University, Piscataway, New Jersey, 08854, USA*
[2] *Hubbard Theory Consortium, Department of Physics, Royal Holloway, University of London, Egham, Surrey TW20 0EX, UK*

(Dated: January 27, 2020)

This paper studies the two-channel Kondo lattice in the large-N limit at half-filling. In this model, the continuous channel-symmetry is spontaneously broken, forming a channel-ferromagnet in which one conduction channel forms a Kondo insulator, while the other remains conducting. The paper discusses how this ground-state can be understood using the concept of *order fractionalization*, in which the channel magnetization breaks up into an emergent spinor order parameter. By integrating out the fermions we derive an effective action that describes this symmetry breaking and its emergent collective modes. A remarkable observation is that topological defects in the order parameter carry a $U(1)$ flux, manifested in the Aharonov-Bohm phase picked by electrons that orbit the defect. By studying the effective action, we argue that the phase diagram contains a non-magnetic transition between a large and a small Fermi surface.

I. INTRODUCTION

The two-channel Kondo impurity and lattice models have a long history. The impurity version of this model was introduced by Blandin and Nozières,[1] who demonstrated that both the weak and strong-coupling fixed points of this model are unstable, flowing to an intermediate coupling fixed point. This novel fixed point was later studied using Bethe ansatz, [2,3] conformal field theory, [4,5] bosonization, [6,7] numerical renormalization group [8] and Majorana representation [9] establishing it as a quantum-critical ground-state with non-Fermi liquid properties and a fractional residual entropy $S = \frac{1}{2}k_B \ln 2$.

The lattice variant of this model, the two-channel Kondo lattice, was proposed by Cox, [10] as a quadrupolar Kondo description of the heavy fermion superconductor UBe_{13}. Cox argued that the crystal-field-split $5f^2$ ground-state of UBe_{13} is characterized by a non-Kramers Γ_3 doublet, whose degeneracy is protected by cubic crystal symmetry, rather than the time-reversal symmetry of Kramers doublets. The key idea of Cox's model is that the criticality of the single-impurity model will nucleate new forms of order in a lattice environment. Cox's two-channel Kondo lattice also forms the basis of proposed models for the hidden order compound URu_2Si_2, where the entanglement of a magnetic Γ_5 non-Kramers doublet with conduction electrons leads to the formation of a spinorial *hastatic* order parameter. [11]

The two channel Kondo lattice Hamiltonian

$$H = \sum_{a=1}^{2}\sum_{\vec{k}\alpha} \epsilon_{\vec{k}} c^\dagger_{\vec{k}\alpha a} c_{\vec{k}\alpha a} + \sum_{j\alpha\beta}\Big(J_1 c^\dagger_{j\alpha 1}\vec{\sigma}_{\alpha\beta}c_{j\beta 1} + J_2 c^\dagger_{j\alpha 2}\vec{\sigma}_{\alpha\beta}c_{j\beta 2}\Big)\cdot\vec{S}_j, \quad (1)$$

defines the coupling between a lattice of local moments $\vec{S}_j$ with two separate conduction seas, labelled by $a = 1, 2$, with coupling constants J_1 and J_2, respectively. The operator

$$c^\dagger_{ja\alpha} = \frac{1}{\sqrt{\mathcal{N}_s}}\sum_{\vec{k}} e^{-i\vec{k}\cdot\vec{R}_j} c^\dagger_{\vec{k}a\alpha}, \quad (2)$$

creates an electron at site j, channel a, with spin component α. Here $\mathcal{N}_s$ is the number of sites in the lattice. We are particularly interested in the case of the symmetric two channel Kondo model, where $J_1 = J_2$, which has channel exchange symmetry $1 \leftrightarrow 2$. Microscopically, this symmetry has its origins in either time-reversal symmetry, or crystal point-group symmetry. For example, in a quadrupolar Kondo effect, the α are pseudo-spin orbital indices while the "channel" index is actually the spin of scattered electrons, so that channel exchange symmetry is actually time-reversal symmetry. In fact at $J_1 = J_2$, the two channel Kondo lattice develops an $SU(2)$ channel symmetry under which the Hamiltonian is invariant w.r.t. continuous rotations between the two channels.

Two recent developments provide a motivation to return to this model. The recent discovery of a new class of "1-2-20" Praseodymium compounds, with formula $PrTr_2Al_{20}$ (where Tr denotes a transition metal ion Tr= Ti, V) or $PrTr_2Zn_{20}$ (where Tr=Ir, Rh) and a $4f^2$ ground-state appear to form a new realization of Cox's original model. [12,13] Unlike UBe_{13}, the smaller hybridization of the Pr atoms makes it possible to definitively confirm the Γ_3 ground-state of these materials. Moreover, they exhibit a wide variety of exotic ground-states, including triplet superconductivity, which appear consistent with novel patterns of entanglement between the non-Kramers doublets and the conduction sea.

Our second motivation is conceptual. Recent work [14] has proposed an interpretation of the expansion of the Fermi surface associated with the Kondo effect as a manifestation of spin fractionalization. This interpretation allows the Kondo effect to be understood without attributing an anthropomorphic electronic origin to the neutral local moments, whose original origin as microscopic qubits, whether electronic, nuclear or other-

wise, is entirely absent from the Kondo lattice Hamiltonian perspective. One of the interesting consequences of this interpretation, is that it develops the phenomenon of "order fractionalization", in which symmetry-broken ground-states acquire half-integer, spinorial character.

A key property of the two-channel impurity Kondo model, is that its quantum critical ground-state is unstable to a variety of relevant, symmetry-breaking Weiss fields.[4] In the lattice, this incipient quantum criticality gives way to a rich phase diagram of competing phases, providing an ideal laboratory for studying the order fractionalization proposal. Dynamical mean-field theory calculations of the two-channel Kondo lattice have reported an incoherent metal,[15] odd-frequency pairing states as well as antiferromagnetism.[16] Recently, however, there are various indications that the two-channel Kondo lattice also contains a Fermi liquid phase in which the Kondo effect spontaneously develops in one of the channels.[17–22] Experimental support for this phase is provided by the measurements on $PrIr_2Zn_{20}$.[12] At high temperatures, this material displays non-Fermi liquid properties, with temperature-dependent resistivity $\rho \sim \sqrt{T}$, expected from dilute two-channel Kondo impurities. At lower temperatures, there is a phase transition into a "dome" of Fermi liquid (FL),[12] a strong candidate for the channel symmetry-broken state. At half-filling, this broken symmetry state results in a Kondo insulator in one channel, leaving behind a conducting metal in the other. This state is the main focus of the current paper.

A. Spin fractionalization and Oshikawa's Theorem

We begin by reviewing the key arguments for fractionalization in the Kondo lattice, before going on to details of our current study. The prototypical single-channel Kondo lattice model is

$$H = \sum_{\vec{k}\alpha} \epsilon_{\vec{k}} c^\dagger_{\vec{k}\alpha} c_{\vec{k}\alpha} + J \sum_{j\alpha\beta} c^\dagger_{j\alpha} \vec{\sigma}_{\alpha\beta} c_{j\beta} \cdot \vec{S}_j. \qquad (3)$$

where

$$c^\dagger_{j\alpha} = \frac{1}{\sqrt{\mathcal{N}_s}} \sum_{\vec{k}} e^{-i\vec{k}\cdot\vec{R}_j} c^\dagger_{\vec{k}\alpha}, \qquad (4)$$

creates an electron at site j. Although this model has a complex phase diagram, for sufficiently large Kondo coupling J it realizes a Fermi liquid (FL) in which the local moments are screened by conduction electrons. Numerical and analytical studies of the model have shown that FL phase is distinct from the original conduction electron FL, for the Fermi surface (FS) is enlarged, as if the local moments have delocalized as electrons. This observation has been placed on rigorous foundation by Oshikawa[23] who argued, using a topological approach, that if the ground state of (3) is a FL, it develops a large FS, in which the volume of the Fermi surface v_{FS} counts

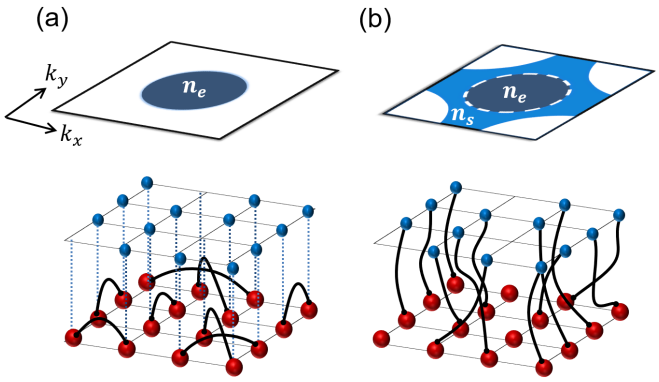

FIG. 1: Schematic representation of a single-channel metallic Kondo lattice (bottom) and corresponding Fermi surface (FS) (top). Local moments and conduction electrons are marked in red/blue. (a) At weak Kondo coupling, the local moments are magnetically correlated and decoupled from the conduction sea, which has a small Fermi surface. (b) For large Kondo interaction, a paramagnetic state is formed in which the electrons and local moments bind into Kondo singlets, forming a large Fermi surface. If there are less electrons than local moments, the unscreened moments form a gas of mobile holes. At half-filling (not shown) Kondo screening may drive a metal into an insulator.

the density of both electrons *and* spins.

$$2\frac{v_{FS}}{(2\pi)^D} = n_e + n_s, \qquad (5)$$

where n_e and n_s are respectively, the density of electrons and local moments per unit cell.

At half-filling, the expansion of the FS to fill the entire Brillouin zone leads to a Kondo insulator. One of the ways to visualize this state is to consider the strong coupling limit, where J is much larger than the bandwidth W of the conduction electrons. When the number of spins and conduction electrons are equal, a local singlet forms at each site, with an insulating gap of size J. Hole doping away from half filling (Fig. 1) then gives rise to a small hole-like Fermi surface of heavy electrons. The volume of the FS counts both electrons and spins.

From a traditional stand-point, the FL phase and Kondo insulating phase of the Kondo lattice are the renormalized counterparts of a FL and a band insulator, respectively. From this traditional perspective, the Kondo lattice Hamiltonian (3) is the result of a Wilsonian renormalization of an Anderson lattice model, which describes hybridization between non-interaction c-electrons and f-electrons with on-site Hubbard interaction U_0

$$H = \sum_k \epsilon_k c^\dagger_{k\alpha} c_{k\alpha} + \sum_j [V_0 (c^\dagger_{j\alpha} f_{j\alpha} + h.c.) + U_0 n^f_{j\uparrow} n^f_{j\downarrow}]. \qquad (6)$$

In the non-interacting limit the Anderson model has a large FS and as long as the interaction U can be switched on adiabatically, forming a Landau Fermi liquid, the FS volume will be unaffected.[24]

However, the process of taking the low-energy limit of the Anderson model projects out empty and double-occupancy of f-electrons (corresponding to the lower and upper Hubbard f-bands), reducing the four-dimensional Hilbert space of the physical electrons f_j to the two-dimensional Hilbert space of the local moment $\vec{S}_j$. The final Kondo model contains no trace of the electronic origin of its local moments. Yet despite this irreversible loss of Hilbert space, *emergent* f-electron fields re-appear at low-energies to expand the FS. Indeed, the high-energy origin of the local moments is entirely irrelevant. The local moments could conceivably even be nuclear in origin, antiferromagnetically coupled to electrons via a hyperfine interaction, which if sufficiently large to overcome nuclear magnetism, would also give rise to a large Fermi surface. This extreme example makes it clear that the f-electrons which develop in the Kondo lattice are emergent, independently of the spins' original microscopic origin.

The large-N mean-field theory using the Abrikosov fermion representation of the spin

$$S_{\alpha\beta}(j) \to f^\dagger_{j\alpha}\left(\frac{\vec{\sigma}}{2}\right)_{\alpha\beta} f_{j\beta}, \tag{7}$$

provides a simple interpretation of these results, [25,26] predicting that at low energies the product of local moment and conduction electron operators behaves as an emergent f-electron field

$$J(\vec{\sigma}_{\alpha\beta}\cdot\overbrace{\vec{S}})c_\beta = V\hat{f}_\alpha. \tag{8}$$

Here, the horizontal line contracting the spin and the fermion implies that at long times, this combination acts as a single composite fermion.

Eq. (8) can be regarded as an operator product identity in the sense that the composite expression on the left can be replaced by the expression on the right in long-time correlation functions. The emergent amplitude V and fermion f are only defined modulo a $U(1)$ phase; an internal gauge degree of freedom that implements the elimination of charge fluctuations of the f-electrons. In the Kondo ground state the internal gauge field locks to the external electromagnetic gauge field, providing the emergent f electrons with an effective electromagnetic charge, which contributes to the FS volume.

Re-inserting Eq. (7) back into Hamiltonian (3), we see that the formation of the fermionic bound-state implies that the low energy physics of a Kondo lattice is described by an Anderson model (6) with hybridization V and an interaction $U \to 0$ that is zero in the large N limit. [27] However, if this behavior is independent of the high energy origin of the Kondo physics (whether it describes an electronic or a nuclear spin), we are obliged to interpret the equations (7) and (8) as a fractionalization of the Kondo spin into emergent f-electrons. While the mean-field theory is only reliable in the large-N limit, recent numerical renormalization group (NRG) studies have shown that this interpretation applies to the Kondo impurity even for the case of spin-1/2 $SU(2)$ spins. [14]

B. Order fractionalization and Two-Channel Kondo Lattice

The spin-fractionalization interpretation of the Kondo effect raises fascinating questions when applied to the two-channel Kondo lattice (Eq. 1). A formal application of Oshikawa's topological argument to this model simply leads to the conclusion that the total FS volume of the two channels is expanded by the spins, i.e

$$n_{e1} + n_{e_2} + n_s = \frac{2}{(2\pi)^3}(v^{(1)}_{FS} + v^{(2)}_{FS}). \tag{9}$$

However, in order to form a Fermi liquid, the two channel Kondo lattice needs to break the channel symmetry responsible for non-Fermi liquid behavior. Blandin-Nozieres scaling arguments suggest that if $J_1 = J_2 + \epsilon$, the asymmetry becomes relevant, and the Kondo effect and the FS expansion will develop exclusively in the strongest channel. In this channel asymmetric state,

$$\begin{aligned} n_{e1} + n_s &= \frac{2}{(2\pi)^3} v^{(1)}_{FS}, \\ n_{e2} &= \frac{2}{(2\pi)^3} v^{(2)}_{FS}. \end{aligned} \tag{10}$$

and if $n_{e1} + n_s = 2$, a Kondo insulator forms exclusively in channel one. Since the second channel remains conducting, we shall refer to this state as a "half Kondo insulator". Now suppose we restore the channel symmetry by sequentially taking $\epsilon \to 0$ at each site in the lattice. Those sites where the channel symmetry is restored will nevertheless feel a channel asymmetry derived from the channel polarization of the Kondo singlets at neighboring sites. Like the Weiss field in a magnet, this effect has the potential to preserve the channel magnetization in the ground-state, even when $\epsilon = 0$ has been restored to zero at every site. Providing the Weiss fields are channel-ferromagnetic, the "half Kondo insulator" will survive the restoration of channel symmetry. This then is an argument for the development of a spontaneous broken channel symmetry.

In this paper we examine this argument within the large N expansion. Our results confirm the stability of the "channel ferromagnet", a state with spontaneously broken channel symmetry and a "channel magnetization"

$$\vec{M}(x_j) = \left\langle c^\dagger_{ja\beta}\vec{\tau}_{aa'}\left(\vec{\sigma}_{\beta\delta}\cdot\vec{S}_j\right)c_{ja\delta}\right\rangle, \tag{11}$$

Here, $\vec{\tau} = (\tau_1, \tau_2, \tau_3)$ are a set of Pauli matrices in the channel space. $\vec{M}$ forms a vector in the channel Bloch sphere, indicating with which channel (or their linear combination) the spin forms the spin-singlet.

However, the channel symmetry breaking co-exists with the spin-fractionalization of the Kondo effect. In the case where $J_1 > J_2$, the fractionalization of the spins involves the formation of a bound-state in channel one,

$$J(\vec{\sigma}_{\alpha\beta}\cdot\overbrace{\vec{S}})c_{1\alpha} = V\hat{f}_\alpha. \tag{12}$$

However, for $J_1 = J_2$ the presence of a perfect $SU(2)$ channel symmetry implies that in the general channel-symmetry broken state,

$$J(\vec{\sigma}_{\alpha\beta} \cdot \overbrace{\vec{S}}) c_{a\alpha} = V z_a \hat{f}_\alpha. \tag{13}$$

where z_a is two component unit spinor. Hence, the hybridization of the two-channel Kondo lattice is now a *two-component spinor* $V_a = V z_a$. The resulting channel magnetization $\vec{M}$ can then be represented in terms of a fractionalized spinorial order parameter $z(x)$

$$\vec{M}(x) \propto z^\dagger(x) \vec{\tau} z(x). \tag{14}$$

The development of an associated insulating behavior in one channel, implies that this is more than a simple CP^1 representation of the channel magnetization. Conventional broken symmetries give rise to local, symmetry breaking scattering potentials, such as the pairing field of an s-wave superconductor, or the Weiss field of a ferromagnet (Fig. 5a). On length-scales larger than the order-parameter coherence length ξ, the corresponding electron self energy is local, e.g

$$\Sigma_{\alpha\beta}(1,2) = M_{\alpha\beta}(1) \delta_\xi(1-2) \tag{15}$$

where $\delta_\xi(1-2)$ is a delta-function, coarse-grained on the scale of ξ. While we can formally decompose $M_{\alpha\beta} \equiv \vec{M} \cdot \tau_{\alpha\beta} = V_\alpha \bar{V}_\beta$ as a CP^1 product of spinors, in a conventional ordering process the two spinors are confined, and always act together at a single space-time point, as a vectorial Weiss field.

However, in the two channel Kondo lattice, the channel magnetization does not create a local scattering potential. Instead, the electrons scatter resonantly off the screened local moments, a process represented by the many-body hybridization with the f-fields that arise from the Kondo spin-fractionalization. The electron self-energy that this gives rise to, is highly non-local in space-time, a self energy of the schematic form

$$\Sigma_{\alpha\beta}(1,2) = V_\alpha(1) G_f(1-2) \bar{V}_\beta(2), \tag{16}$$

where $G_f(1-2)$ is the bare f-electron propagator between 2 and 1 (Fig. 5b). To form an insulator, the unhybridized f-band must lie within the insulating gap, and the consequential absence of inelastic scattering at these energies guarantees that the Green's function $G_f(1-2)$ is infinitely retarded in space and time, so there is no coherence length-scale beyond which the two spinor variables $V(1)$ and $\bar{V}(2)$ coalesce into a single vector order parameter. In this way, the channel magnetization has fractionalized.

C. Collective modes and Topological Defects

Another key interest in this paper is to examine gapless modes of the two-channel Kondo lattice in the channel symmetry broken phase, corresponding to the Goldstone rotations of the three Euler angles of the spinor order parameter. We shall show that as in the single-channel Kondo lattice, one of these modes is absorbed by a Higgs mechanism that locks the $U(1)$ gauge fields associated with the fractionalized f-electron to the external electromagnetic field, giving the f-electrons physical charge, and driving the large electronic FS.

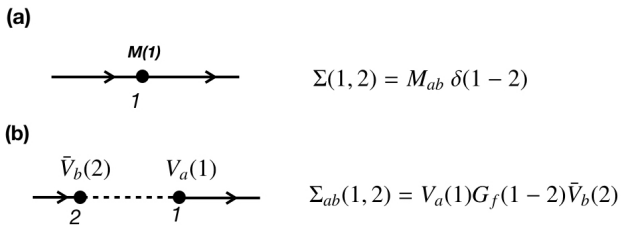

FIG. 2: Feynman diagrams for (a)local scattering off a conventional Weiss order parameter field $M(1)$ and (b) resonant scattering off a fractionalized order parameter, where the dotted line represents the propagator of the fractionalized spin.

A key finding, is that the channel magnetization $\vec{M}$ admits topological configurations: skyrmions in 2 dimensions or 'hedgehog' instantons in 2+1 dimensions, which couple to the underlying gauge charges in the system. These topological excitations modify the electronic spectrum. When the Kondo temperature becomes sufficiently weak, the proliferation of such hedgehog defects is expected to lead to a 'quantum disordered' phase, in which the coherence between the gauge field of spinons and the external field is destroyed and the ground state has a small FS.

The structure of the paper is as follows. In section II we use the large-N mean-field theory to study the ground state of the two-channel Kondo lattice. In subsection II D we show that a natural description of the ground state in the ordered phase is provided by the concept of order fractionalization. [14] In section III, we integrate out the fermions and derive an effective action that describes collective excitations of the system, including the Higgs mechanism and the small to large FS transition mentioned above. Finally, we conclude the paper in section IV and list a number of open questions. A number of appendices are included to provide additional derivations and details used in the paper.

II. MEAN FIELD THEORY OF THE TWO-CHANNEL KONDO LATTICE

We consider a two-channel Kondo lattice, represented by Hamiltonian (1). As written, the channel index is an orbital quantum number, while the local degrees of freedom are spins. We note that in the equivalent quadrupolar formulation of the two-channel Kondo model proposed by Cox, $\vec{S}_j$ represents a non-Kramers doublet. In

this case, α is a quadrupole index while the channel index corresponds to the "up" and "down" spins of the conduction sea. To develop a controlled mean field theory, we extend the number of spin components from 2 to N by taking the spins from an irreducible representation of $SU(N)$ instead of $SU(2)$. This generalized version of the model uses the Coqblin-Schrieffer form of the interaction [25,28]

$$H = \sum_{\vec{k}a\alpha} \epsilon_{\vec{k}} c^\dagger_{\vec{k}a\alpha} c_{\vec{k}a\alpha} + J \sum_{ja\alpha\beta} c^\dagger_{ja\alpha} c_{ja\beta} S_{\beta\alpha}(j). \tag{17}$$

Here, $S_{\beta\alpha}(j)$ are representations of generators of the $SU(N)$ group. This symmetric two channel Kondo lattice model possesses an $SU_{spin}(N) \times SU_{channel}(2) \times U_{charge}(1)$ symmetry. We shall use an Abrikosov fermion representation of the $SU(N)$ spin operators,

$$S_{\alpha\beta} = f^\dagger_\alpha f_\beta - \frac{Q}{N}\delta_{\alpha\beta}, \tag{18}$$

subject to the constraint

$$n_f = f^\dagger_\alpha f_\alpha = Q, \tag{19}$$

where Q is an integer. To develop a controlled large-N expansion for the Kondo lattice, the coupling constant is rescaled by a factor of $1/N$ to guarantee that each term in the Hamiltonian scales extensively with N. In terms of the Abrikosov representation, the Hamiltonian becomes

$$H = \sum_{\vec{k}a\alpha} \epsilon_{\vec{k}} c^\dagger_{\vec{k}a\alpha} c_{\vec{k}a\alpha} - \frac{J}{N} \sum_{ja\alpha\beta} (c^\dagger_{ja\alpha} f_{j\alpha})(f^\dagger_{j\beta} c_{ja\beta}) \tag{20}$$

$$+ \sum_j \lambda_j (n_{fj} - Q) \tag{21}$$

where the Lagrange multiplier λ_j is introduced to impose the constraint $n_f = Q$ at each site. The Abrikosov factorization of the spin operator permits one to write the partition function as a path integral

$$Z = \mathrm{Tr}\left[e^{-\beta H}\right] = \int \mathcal{D}[\bar{c}, c, \bar{f}, f, \lambda] e^{-S}. \tag{22}$$

Inside the path integral the interaction can be decoupled in each channel using a Hubbard-Stratonovich transformation, [26,29]

$$-\frac{J}{N}\sum_{\alpha\beta}(c^\dagger_{ja\alpha} f_{j\alpha})(f^\dagger_{j\beta} c_{ja\beta}) \rightarrow \left[(c^\dagger_{ja\alpha} f_{j\alpha}) V_{aj} + \mathrm{H.c}\right] + \frac{N}{J}|V_{aj}|^2,$$

where the "hybridization" field V_a is to be integrated over inside the path integral,

$$Z = \int \mathcal{D}[\overline{c}, c, \overline{f}, f, \overline{V}_a, V_a, \lambda]\ e^{-S}$$

with the action

$$S = \int_0^\beta \mathrm{d}\tau \left\{ \sum_{\vec{k}a} \overline{c}_{\vec{k}a}(\partial_\tau + \epsilon_{\vec{k}}) c_{\vec{k}a} + \sum_{j\alpha} \overline{f}_j(\partial_\tau + \lambda_j) f_j + \sum_{ja}\left[\overline{c}_{ja}(V_{aj} f_j) + (\bar{f}_j \bar{V}_{aj}) c_{ja}\right] + \sum_{ja} \frac{N}{J}|V_{aj}|^2 - \sum_j \lambda_j Q \right\}. \tag{23}$$

Here, and in the following the summation over the spin indices $\alpha = 1 \ldots N$ is implicit.

A. Symmetries and Gauge Transformations of the Hamiltonian

The symmetric two-channel Kondo lattice exhibits a number of global and local symmetries: The conduction electrons are invariant under global $U(1) \times SU(2)$ rotations in channel space

$$c_{ja} \rightarrow g_{aa'} c_{ja'}, \qquad V_{aj} \rightarrow g_{aa'} V_{a'j}.$$

The f-electrons possess a local $U(1)$ gauge invariance associated with the conserved f-charge $n_f(j) = Q_j$,

$$f_j \rightarrow e^{i\chi_j} f_j, \quad V_{aj} \rightarrow V_{aj}\ e^{-i\chi_j}, \quad \lambda_j \rightarrow \lambda_j(\tau) - i\partial_\tau \chi_j(\tau).$$

In the single-channel Kondo impurity/lattice, this gauge transformation is used to make the hybridization real with the price of transforming the original static λ_j into a dynamical, time-dependent field. [26]

It is convenient to represent the hybridization fields as a spinor

$$\begin{pmatrix} V_1(j,\tau) \\ V_2(j,\tau) \end{pmatrix} \equiv V(j,\tau) \begin{pmatrix} z_1(j,\tau) \\ z_2(j,\tau) \end{pmatrix} \tag{24}$$

where $V(j,\tau)$ is a positive real number representing the magnitude of the hybridization and z_1 and z_2 define a

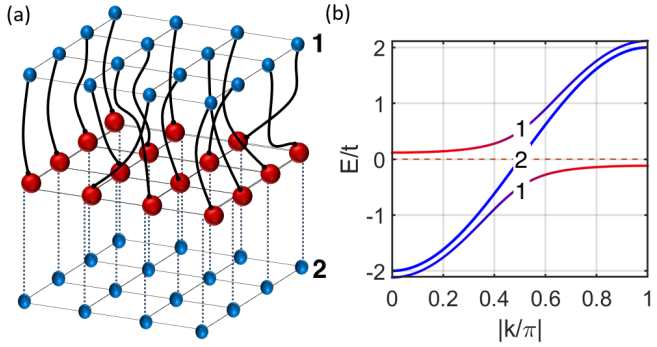

FIG. 3: (a) Channel ferromagnetic state: the localized spins (red) hybridize with one out of two conduction channels (blue). (b) A schematic representation of the band structure in a half Kondo insulator.

unit spinor with $z^\dagger z = |z_1|^2 + |z_2|^2 = 1$ which can be written in terms of Euler angles

$$z \equiv \begin{pmatrix} z_1 \\ z_2 \end{pmatrix} = e^{i\varphi/2} \begin{pmatrix} \cos\theta/2 \\ -e^{i\phi}\sin\theta/2 \end{pmatrix}. \tag{25}$$

Since the underlying channel symmetry is $SU(2)$, the full range of values in this unit spinor involve a double covering of the $SO(3)$ group, incorporated by doubling the range of $\varphi \in [0, 4\pi]$.

B. Uniform Mean Field Solution

In the limit $N \to \infty$ the path integral is dominated by the stationary points of the action characterized by static, uniform configurations of the hybridization spinor, such that $V_j = V$, $\theta_j = \theta$, $\phi_j = \phi$, $\varphi_j = \varphi$ and $\lambda_j = \lambda$ are all constant. The overall phase $e^{i\varphi/2}$ in the hybridization can be absorbed by a gauge transformation $f_j \to e^{i\varphi/2} f_j$ of the f-electrons. Moreover, by rotating in channel space

$$\begin{pmatrix} c'_{k1} \\ c'_{k2} \end{pmatrix} = \begin{pmatrix} \cos\theta/2 & e^{-i\phi}\sin\theta/2 \\ -e^{i\phi}\sin\theta/2 & \cos\theta/2 \end{pmatrix} \begin{pmatrix} c_{k1} \\ c_{k2} \end{pmatrix}, \tag{26}$$

the mean-field action becomes

$$S = \int_0^\beta \mathrm{d}\tau \sum_{\vec{k}\alpha} \left\{ (\bar{c}'_{\vec{k}1}, \bar{f}_{\vec{k}}) \left[\partial_\tau + \begin{pmatrix} \epsilon_{\vec{k}} & V \\ V & \lambda \end{pmatrix} \right] \begin{pmatrix} c'_{\vec{k}1} \\ f_{\vec{k}} \end{pmatrix} + \bar{c}'_{\vec{k}2}(\partial_\tau + \epsilon_{\vec{k}}) c'_{\vec{k}2} + \mathcal{N}_s \left(\frac{NV^2}{J} - \lambda Q \right) \right\}, \tag{27}$$

where we have defined $f_{\vec{k}} = \frac{1}{\sqrt{\mathcal{N}_s}} \sum_j f_j e^{i\vec{k}\cdot\vec{R}_j}$. For the case where $Q = N/2$ and a particle-hole symmetric conduction band, we have $\lambda = 0$ by the symmetry.

In this basis, the second conduction electron channel decouples from the f-electrons as shown schematically in Fig. 3(a). The system reduces to a "half Kondo insulator", with a first hybridized channel, forming a fully gapped Kondo insulator with upper and lower bands dispersing according to

$$E^\pm_{\vec{k}} = \frac{\epsilon_{\vec{k}}}{2} \pm \sqrt{\left(\frac{\epsilon_{\vec{k}}}{2}\right)^2 + V^2}, \tag{28}$$

and a second decoupled conduction band with dispersion $\epsilon_{\vec{k}}$. This is shown in Fig. 3(b). In two spatial dimensions, the free energy per site per particle is

$$\frac{F}{\mathcal{N}_s N} = -T \int \frac{\mathrm{d}^2k}{(2\pi)^2} \Big\{ \log\left[1 + e^{-\beta\epsilon_{\vec{k}}}\right] + \sum_\pm \ln\left[1 + e^{-\beta E^\pm_{\vec{k}}}\right] \Big\} + \frac{V^2}{J}. \tag{29}$$

The solution for the magnitude of the hybridization V can be obtained self consistently from the stationarity condition

$$\frac{1}{\mathcal{N}_s N}\frac{\delta F}{\delta V^2} = \frac{1}{J} - \int \frac{\mathrm{d}^2k}{(2\pi)^2} \left(\frac{f(E^-_{\vec{k}}) - f(E^+_{\vec{k}})}{2\sqrt{\left(\frac{\epsilon_{\vec{k}}}{2}\right)^2 + V^2}} \right) = 0,$$

where $f(E) = [1 + e^{\beta E}]^{-1}$ is the Fermi-Dirac function. Using a constant density of states $\rho(\epsilon) = \rho\theta(4t - |\epsilon|)$, where $\rho = 1/8t$, we can solve for the hybridization at $T = 0$, giving

$$\frac{1}{J} = \rho \int_{-4t}^{4t} \frac{d\epsilon}{\sqrt{\epsilon^2 + 4V^2}} = 2\rho \sinh^{-1}\left(\frac{2t}{V}\right) \tag{30}$$

or

$$V^{-1} = 4\rho \sinh\left(\frac{1}{2\rho J}\right), \tag{31}$$

or $V = 4te^{-\frac{1}{2\rho J}}$ in the large band-width limit. The ground state energy is plotted for different hybridization strengths for a constant density of states and for the exact density of states for a conduction band with nearest neighbor hopping in figure 4(a). The minimum of the

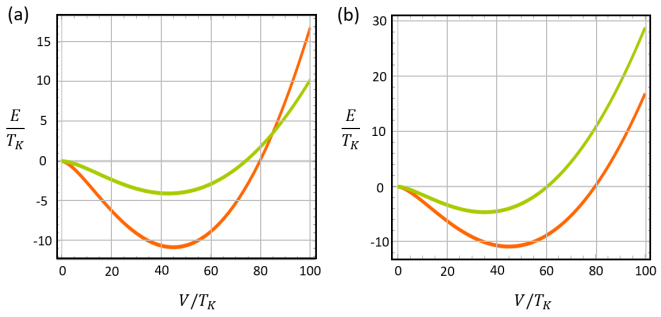

FIG. 4: (a) Ground state energy of a two-dimensional half-Kondo insulator state using constant (green) and exact (red) density of states. (b) Comparison of ground state energies of the half-Kondo insulator (channel ferromagnet in red) and the staggered hybridization solution (channel antiferromagnet in green).

ground state energy corresponds to the actual hybridization strength.

Similarly, the mean-field transition temperature $T = T_K$ is determined by

$$\frac{1}{J\rho} = \int_{-4t}^{4t} d\epsilon \frac{1/2 - f(\epsilon)}{\epsilon} = \ln\left[\frac{4t}{T_K}\left(\frac{e^{-\psi(1/2)}}{2\pi}\right)\right] \quad (32)$$

From which it follows that

$$T_K = 4t\overbrace{\left(\frac{e^{-\psi(1/2)}}{2\pi}\right)}^{1.13} e^{-\frac{1}{\rho J}} = \left(\frac{1}{3.53}\right)\left(\frac{V^2}{t}\right), \quad (33)$$

where the integral is derived in appendix 16A in the book by Coleman [26]. Note that while the direct gap is determined by V, the mean-field transition temperature, or Kondo temperature is determined by the much smaller, indirect gap, $\Delta_g = V^2/2t = \frac{3.53}{2}T_K$. In Appendix A we compare this half Kondo insulator state with a channel symmetry breaking pattern, for which the hybridization is staggered in channel space. The ground state energies of the half Kondo insulator state and the staggered hybridization state are compared in figure 4(b). We see that the half-Kondo insulator state is energetically stable with respect to the channel antiferromagnet for all values of the coupling. This is an important result, for it confirms that the channel Weiss fields acting between different spin sites are ferromagnetic in nature at half filling.

C. Kondo-Heisenberg system

So far, we have assumed that the spins do not directly interact with each other and each spin is a self-conjugate $Q = N/2$ fermionic representation of $SU(N)$, so that together with a half-filled conduction band the whole system has particle-hole symmetry. More generally, the Kondo coupling induces an RKKY interaction amongst the spins, which is generically long-ranged and varies in space. Assuming that the system does not magnetically order at low temperatures, in the rest of the paper, we generalize our model $H \to H + H_{\rm AFM}$ to include effects of a frustrated antiferromagnetic interaction among the spins:

$$H_{\rm AFM} = \sum_{i,j} J_{ij}^H \vec{S}_i \cdot \vec{S}_j. \quad (34)$$

In the SU(N) limit, using the Abrikosov fermion representation, and applying the constraint this leads to

$$H_{\rm AFM} = -\frac{1}{N}\sum_{(i,j),\alpha,\beta} J_{ij}^H \left(f_{i\alpha}^\dagger f_{j\alpha}\right)\left(f_{j\beta}^\dagger f_{i\beta}\right) \quad (35)$$

which can be decoupled by a Hubbard-Stratonovitch transformation $t_{ij} = |t_{ij}|\, e^{i\varphi_{ij}}$

$$H_{\rm AFM} \to \sum_{(i,j)}\left\{\frac{N|t_{ij}|^2}{J_{ij}^H} + \left[\left(|t_{ij}|\, e^{i\varphi_{ij}} f_{i\alpha}^\dagger f_{j\alpha} + h.c.\right)\right]\right\}. \quad (36)$$

with an implied summation over the repeated spin variables $\alpha \in [1, N]$. We assume that the underlying spin fluid is a $U(1)$ spin liquid, characterized by a spinon Fermi surface. The phase factor

$$e^{i\varphi_{ij}} \sim \exp\left[i\int_{\vec{R}_j}^{\vec{R}_i} \vec{A}^f \cdot \vec{dl}\right], \quad (37)$$

is in fact the Peierls substitution of a slowly varying $U(1)$ gauge degree of freedom. While the phases φ_{ij} themselves are gauge-dependent, e.g. by a redefinition of f_j that leaves the spin representation unaffected,

$$f_j \to f_j e^{i\chi_j}, \qquad \varphi_{ij} \longrightarrow \varphi_{ij} - \chi_i + \chi_j, \quad (38)$$

the sum of the phases around plaquettes is gauge-invariant and corresponds to the $U(1)$ gauge flux through the plaquettes: [30]

$$\sum_{(i,j)\in\square} \varphi_{ij} \equiv \oint_\square \vec{A}^f \cdot \vec{dl} = \Phi_f \quad (39)$$

The combination of the magnitude/phase of t_{ij} gives rise to a dispersion for the spinons ϵ_k^f so that the momentum-space Hamiltonian is

$$H_{\rm AFM} \to \sum_{ij} \frac{|t_{ij}|^2}{J_{ij}^H} + \sum_{k\alpha} \epsilon_k^f f_{k\alpha}^\dagger f_{k\alpha}. \quad (40)$$

The simplest case is a nearest-neighbor tight-binding lattice of $q = 1/2$ moments and no flux per plaquette $\sum_{(i,j)\in\square}\varphi_{ij} = 0$, with the 2D spinon dispersion

$$\epsilon_k^f = -2t_f(\cos k_x + \cos k_y). \quad (41)$$

If we allow the gauge fields $\vec{A}^f$ to vary slowly in space, then the coarse-grained action of the f-electrons takes the form [30]

$$S_f = \int d^3x dt \bar{f} \left[-i\partial_t + \lambda + \epsilon^f(-i\vec{\nabla} - \vec{A}) \right] f \qquad (42)$$

where we have replaced $\partial_\tau \to -i\partial_t$. This action is invariant under the gauge transformation $f \to e^{i\chi} f$ and

$$\lambda \to \lambda - \partial_t \chi, \qquad \vec{A}^f \to \vec{A}^f + \vec{\nabla}\chi, \qquad (43)$$

allowing us to combine $A^f_\mu \equiv (-\lambda, \vec{A}^f)$ into a single $U(1)$ gauge field that transforms as $A^f_\mu \to A^f_\mu + \partial_\mu \chi$. Hence, variations of $U(1)$ gauge on top of the mean-field background can be taken into account by the by the minimal coupling $-i\partial_\mu \to -i\partial_\mu - A^f_\mu$ or $p_\mu \to p_\mu - A^f_\mu$.

D. Order fractionalization

In the two channel case, the f-electrons can be integrated out and the self-energy for the conduction electrons has the form

$$\Sigma_{ab}(\vec{k}, \omega) = \frac{V_a \bar{V}_b}{\omega - \epsilon^f_k}, \qquad (44)$$

where $a, b = 1, 2$ are the channel indices of the conduction electrons. Writing $V_a = V z_a$, where $z^\dagger z = 1$ is a unit spinor, we have

$$\Sigma_{ab}(\vec{k}, \omega) = \frac{V^2}{\omega - \epsilon^f_k} z_a \bar{z}_b = \frac{V^2}{\omega - \epsilon^f_k} \left(\frac{1 + \vec{n}\cdot\vec{\tau}}{2} \right)_{ab} \qquad (45)$$

where $\hat{n} = z^\dagger \vec{\tau} z$. Were it not for the strong frequency dependence of this self-energy, we could simply regard this term as a Weiss scattering field created by a channel magnetization.

For a slowly varying order parameter, the self-energy becomes

$$\Sigma_{ab}(2;1) = V_a(2) G_f(2-1) \bar{V}_b(1). \qquad (46)$$

where $G_f(2-1)$ is the bare propagator of an f-electron from 1 to 2. To make the state insulating, the unhybridized f-band must cut the Fermi energy to repel the conduction band from the Fermi energy. This causes $G_f(2-1)$ to develop infinite range correlations in time, so that we are forced to regard the spinors $V_a(2)$ and $\bar{V}_{a'}(1)$ as independent variables.

Part of this propagator is the dynamic phase accumulated from 1 to 2. For example, for non-dispersing f-electrons,

$$G_f(2-1) \sim \exp\left[-i \int_{t_1}^{t_2} \lambda(t') dt' \right]. \qquad (47)$$

At particle-hole symmetry $\lambda = 0$, the self-energy in real space/time becomes

$$\Sigma_{ab}(2;1) = -\frac{\delta_{\vec{x}_2, \vec{x}_1}}{2} V_a(\tau_2) \mathrm{sgn}(\tau_2 - \tau_1) \bar{V}_b(\tau_1). \qquad (48)$$

More generally however, the f-state will develop a dispersion due to the magnetic interaction

$$G_f(\vec{k}, \omega) = \frac{1}{\omega - \epsilon^f_k}. \qquad (49)$$

In general, $\epsilon^f_{\vec{k}}$ has zeros and will cut the Fermi energy on a surface $\{S_0 : \vec{k} = \vec{k}_0\}$. Since the self-energy diverges at $\omega = 0$ on this surface, it follows that S_0 corresponds to the zeros of the conduction electron propagator. The corresponding real-time propagator will take the form

$$G_f(\vec{x}, t) = \frac{e^{ik_0 x}}{x - v^f_{\vec{k}_0} t} \qquad (50)$$

where $\vec{k}_0$ is at the point on the null surface S_0 with normal parallel to the separation vector $\vec{x} = x\hat{n}$, so that

$$\Sigma_{ab}(2;1) = V_a(2) \frac{e^{ik_0 |\vec{x}_2 - \vec{x}_1|}}{|\vec{x}_2 - \vec{x}_1| - v^f_{\vec{k}_0}(t_2 - t_1)} \bar{V}_b(1) \qquad (51)$$

In conventional broken symmetry phases, the self-energy is local on a scale of the coherence length: but here, the resonant scattering process through an intermediate spin-fluid means that the initial and final hybridization events $V_\beta(1)$ and $\bar{V}_\beta(2)$, can be arbitrarily separated in space and time. This is a key signature of the fractionalization. Notice that while the fermion field f and the hybridization order parameters appearing here, are only defined modulo a gauge transformation, the self-energy $\Sigma(2-1)$ is invariant under these transformations.

III. COLLECTIVE EXCITATIONS

A. The soft modes

Within the large-N mean-field theory, the Kondo coupling reduces to a hybridization between Abrikosov fermions and the two conduction bands, described by an spinor $V_a(x, \tau)$ in the Hamiltonian density

$$\mathcal{H}_{int} \to \frac{V^2}{J_K} + (c^\dagger_a V_a f + h.c.). \qquad (52)$$

At high temperature, the hybridization is strongly fluctuating, but once $T \lesssim T_K$, the hybridization spinor acquires a non-zero expectation value $V_a \neq 0$. Longitudinal fluctuations in the magnitude of V_a are massive and gapped, but (transverse) fluctuations in the direction of the V_a spinor develop soft modes. This physics is conveniently shown by writing $V_a(x, \tau) = V z_a(x, \tau)$ and

$$z(x, \tau) = \mathrm{g}(x, \tau) \begin{pmatrix} 1 \\ 0 \end{pmatrix}, \qquad (53)$$

where $\mathrm{g} \in U(2)/U(1) \sim SU(2)$. We can parameterize g by the three Euler angles

$$\mathrm{g}(x, \tau) = e^{i\phi\tau_3/2} e^{i\theta\tau_2/2} e^{i\varphi\tau_3/2}. \qquad (54)$$

By integrating out the fermions, we can derive a long-wavelength effective action that describes the spontaneous symmetry breaking from this fluctuating phase to the channel ferromagnetic ground state.

In the following, we consider a long-wavelength ($k \sim 0$) approximation to the model (40) and assume that the spinon dispersion is quadratic near $k \sim 0$. Moreover, we assume a continuum theory of conduction electrons with parabolic dispersions. This combination describes the low-energy limit of the two-channel Kondo-Heisenberg lattice, in presence of both, an external electromagnetic vector potential $A^{\rm ext}$ and an internal gauge potential A^f. That such a continuum Kondo insulator exists, is discussed in Appendix B.

The Hamiltonian density is $\mathcal{H}(x) = \mathcal{H}_0(x) + \mathcal{H}_{int}(x)$ where $\mathcal{H}_{int}$ is given in eq. (52) and $\mathcal{H}_0$ is given by

$$\mathcal{H}_0(x) = C(x)^\dagger \Big[\sum_{\nu=1}^{d} \frac{(p_\nu - eA_\nu^{\rm ext})^2}{2m_c} + ieA_\tau^{\rm ext} - \mu \Big] C(x) + f^\dagger(x) \Big[-\sum_{\nu=1}^{d} \frac{(p_\nu - A_\nu^f)^2}{2m_f} + iA_\tau^f + \lambda \Big] f(x). \quad (55)$$

The Wick rotation of scalar potentials is $A_\tau \to -iA_t$. Note that the effective masses of the c- and f- bands are opposite to one-another, to insure that the hybridized channel is insulating. Here, $p_\nu = -i\partial_\nu$, $C = (\, c_1,\ c_2\,)^T$ and the spin indices $\alpha \in [1, N]$ have been suppressed. The second line describes a gapless $U(1)$ spin-liquid. The internal gauge field A^f arises from decoupling the Heisenberg magnetic interaction between f-electrons (spinons) as described in section (II C)[30]. The temporal and spatial variations of the hybridization in Eq. (53) can be absorbed into the C electrons by a $C \to \mathbb{g}C$ transformation. This leads to

$$C^\dagger \partial_\mu C \to C^\dagger [\partial_\mu + \mathbb{g}^\dagger \partial_\mu \mathbb{g}] C, \quad (56)$$

and motivates defining a gauge connection $\mathbb{A}_\mu^C \equiv -i\mathbb{g}^{-1}\partial_\mu \mathbb{g}$ which can be expanded $\mathbb{A}_\mu^C = \frac{1}{2}\sum_a \Omega_\mu^a \tau^a$ in terms of Pauli matrices τ^a, where Ω_μ^a are the components of the angular velocity associated with the Euler rotations. This gauge connection can be combined with the external electromagnetic gauge potential as $\mathbb{A} = \mathbb{A}^C - \tau^0 A^{\rm ext}$. Setting $e = 1$, the Lagrangian in imaginary time is

$$\mathcal{L} = \bar{C}\Big[(\partial_\tau - \mu)\mathbb{1} + i\mathbb{A}_\tau - \frac{1}{2m_c}\sum_{\nu=1}^{d}(\partial_\nu \mathbb{1} + i\mathbb{A}_\nu)^2\Big] C + \bar{f}\Big[(\partial_\tau + \lambda) - iA_\tau^f + \frac{1}{2m_f}\sum_{\nu=1}^{d}(\partial_\nu - iA_\nu^f)^2\Big] f + V[c_1^\dagger f + f^\dagger c_1] + iA_\tau^{\rm ext} n_c + iA_\tau^f Q. \quad (57)$$

Here we have added two constraint terms, a term $iA_\tau^{ex} n_c$ which account for the coupling of the fluctuations in the electromagnetic potential to the positive charge density of the ionic background n_c, ensuring overall charge neutrality and the term $iA_\tau^f Q$ which imposes the constraint $n_f = Q$ at each site. These terms ensure that when we carry out a gradient expansion, terms linear in the gauge potentials vanish. From equation (57), the action of the ungapped conduction electrons is given by

$$\mathcal{L}_{c2} = \bar{c}_2 \Big[\partial_\tau - i(A_0 + \tfrac{1}{2}\Omega_\tau^3) + \frac{1}{2m_c}\big[-i\nabla_a - (A_a + \tfrac{1}{2}\Omega_a^z)\big]^2\Big] c_2. \quad (58)$$

One of the interesting physical consequences of this action, is that the propagation of the ungapped electrons in channel 2 picks up the Berry phase associated with the spinor hybridization, so that the vector potential acting on the ungapped electrons in channel 2 acquires an additional component associated with the Berry phase of the spinor field,

$$A_\mu^{ext} \to A_\mu^{ext} + \tfrac{1}{2}\Omega_\mu^z \quad (59)$$

where $\Omega_\mu^z = -2iz^\dagger \partial_\mu z$ is the Berry connection of the order parameter.

B. Effective action

The effective action for the gauge fields

$$Z = \int [\mathcal{D}A^f \mathcal{D}A^{\rm ext} \mathcal{D}A^{SU(2)}] e^{-S_{\rm eff}} \quad (60)$$

can be obtained by integrating out the fermions (Appendix C). A caricature of the long-wavelength action $S_{\rm eff}$ can be derived from a Landau-Ginzburg theory of the hybridization:

$$\frac{\mathcal{L}_{\rm 2CK}}{N} \sim \frac{\hbar^2}{2m}\left|(-i\partial_\mu + [A_\mu^{ext} - A_\mu^f])V\right|^2 + \frac{b}{2}\left(|V|^2 - V_0^2\right)^2 \quad (61)$$

The minimal coupling of the hybridization to the difference field $A_\mu^{ext} - A_\mu^f$, is enforced by the gauge invariance of the hybridization terms $(c^\dagger V f) + \text{H.c.}$ Under a gauge transformation $c \to e^{i\theta}c$, $f \to e^{i\chi}f$, $V \to e^{i(\theta-\chi)}V$, so that V has the same electrical charge as a conduction electron, but the opposite gauge charge to an f-electron.

At long distances, we may ignore amplitude fluctuations. Substituting $V = V_0 z$, where

$$z = \mathbb{g}\begin{pmatrix}1\\0\end{pmatrix} = e^{i\phi\tau_3/2}e^{i\theta\tau_2/2}e^{i\varphi\tau_3/2}\begin{pmatrix}1\\0\end{pmatrix}.$$

we obtain

$$\mathcal{S}_{\rm eff} = \int d^{d+1}x \mathcal{L}_{\rm 2CK}$$
$$\mathcal{L}_{\rm 2CK} \sim \frac{1}{2g}\Big[\left(\partial_\mu \vec{n}\right)^2 + \left(\Omega_\mu^z - 2[A_\mu^{\rm ext} - A_\mu^f]\right)^2\Big]. \quad (62)$$

where the implicit sum on $\mu \in [0, d]$ runs over all space-time dimensions. Here,

$$\vec{n} = z^\dagger \vec{\tau} z = (-\sin\theta\cos\phi, \sin\theta\sin\phi, \cos\theta), \quad (63)$$

is the channel magnetization, while

$$\Omega^z_\mu = [\partial_\mu\varphi + \partial_\mu\phi\cos\theta] = -i2z^\dagger\partial_\mu z. \tag{64}$$

is the angular velocity of the spinor order about its principle z axis and $g^{-1} = \frac{\hbar^2}{4m}V_0^2$.

Without the gauge coupling, this Lagrangian is the principal chiral field model, describing the evolution of a spinor order parameter in space-time. [31] However, the coupling of the difference gauge field of $A^{ext}_\mu - A^f_\mu$ to rotations about the principle "z" axis of the order parameter, "Higgses" the phase fluctuations around the z-axis. The factor of two multiplying the coupling of the difference gauge fields reflects the fact that the channel magnetization as a vector, carries integer channel quantum number whereas the electrons, carry a half-integer channel quantum number, $\tau = 1/2$. A detailed calculation of the effective action to one loop order in the fermions is similar to the calculation of a superfluid stiffness in a superconductor, and involves diagrams of the form depicted in Fig. 6(a). These calculations (see Appendix C) confirm the basic form obtained from the Landau-Ginzburg theory, but with different stiffnesses and mode velocities for rotations parallel and perpendicular to the $\hat{n}$ axis. The full Lagrangian, including the contributions of the gapless electrons in channel 2 is then,

$$\mathcal{L}_{\rm 2CK} = \frac{N}{2g}\Big[\big(\partial_\tau\vec{n}\big)^2 + v_g^2\big(\nabla\vec{n}\big)^2\Big] + \frac{N\Gamma}{2}\Big[\Big(\Omega^z_\tau - 2[A^{\rm ext}_\tau - A^f_\tau]\Big)^2 + v_\Gamma^2\sum_{i=1}^{d}\Big(\Omega^z_i - 2[A^{\rm ext}_i - A^f_i]\Big)^2\Big]$$
$$+\bar{c}_2\left[\partial_\tau - i[A_0 + \tfrac{1}{2}\Omega^3_\tau] + \frac{1}{2m_c}\Big(-i\nabla_a - [A_a + \tfrac{1}{2}\Omega^z_a]\Big)^2\right]c_2 \tag{65}$$

Note that the action scales as N, ensuring that the variance of the fluctuations about the large N limit are of order $O(1/N)$. In the limit that $m_f \gg m_c$, the stiffness and velocity coefficients are given by (see Appendix C)

$$\frac{1}{g} \approx 2\rho\mathcal{Z}, \qquad v_g \approx \frac{v_c}{\sqrt{\mathcal{Z}}} \tag{66}$$

$$\Gamma \approx \frac{\rho}{4}, \qquad v_\Gamma \approx \sqrt{\frac{\pi^2}{2}v_f v_c} \tag{67}$$

Here $\tilde{q}_f = k_F^2/4\pi$ is the density of f-holes, $\rho = m_c/2\pi$ is the conduction electron density of states, $v_c = k_F/m_c$ and $v_f = k_F/m_f$ are the Fermi velocities of the conduction and f-electrons respectively, while

$$\mathcal{Z} = \left[1 + \frac{\rho T_K}{\tilde{q}_f}\Big(1 + \frac{\tilde{q}_f}{\rho_f T_K}\Big)^2\right] \tag{68}$$

is a mass renormalization factor, where $\rho_f = m_f/2\pi$ is the f-electron density of states. Note that in the limit where the Heisenberg coupling is zero $J_H \to 0$, $m_f \to \infty$ and the axial stiffness $(v_\Gamma)^2\Gamma \to 0$ associated with the Higgs term vanishes, whereas the O(3) stiffness associated with the channel magnetization $(v_g)^2/g$, remains finite.

C. The Anderson-Higgs term

To understand the effect of the Anderson-Higgs term in (65) it is useful to first consider the simpler single-channel Kondo lattice [32] where the effective action takes the form

$$\mathcal{L}_{\rm 1CK} = \sum_{\mu=0}^{d}\frac{\Gamma}{2}(\partial_\mu\varphi - 2(A^{\rm ext}_\mu - A^f_\mu))^2, \tag{69}$$

where $\Gamma = N/g$. The scaling dimension of this Γ coupling is $\dim[\Gamma] = d - 1$, making it relevant for $d > 1$. For $d > 1$, in the ground-state, the internal $U(1)$ 'vison' field A^f is phase-locked to the external gauge potential up to a pure gauge and a Meissner effect develops for the difference field $A^{\rm ext}_\mu - A^f_\mu$, excluding the corresponding electromagnetic fields from the sample. By fixing the gauge, we can absorb the φ field into the vison gauge field A^f.

Once the vison and electromagnetic fields lock, the conduction and f electrons respond coherently to the common external electromagnetic field, so the f-electrons acquire charge and now contribute to the Fermi surface (FS) volume. Thus, the development of f-electron charge and the formation of a large FS in the Fermi liquid regime of the Kondo lattice, as required by Oshikawa's theorem [23] are all linked to this Anderson-Higgs effect.

A similar effect occurs in the two channel model, but now, the absorption of the phase φ into the gauge fields leaves behind the (ϕ, θ) variables, which define the direction $\hat{n}(x)$ of the channel magnetization. One of the important distinctions here, is that although the φ field is Higgsed, the Berry phase term of the spinor order is still present, described by the field

$$\Omega^z_\mu \to \partial_\mu\phi\cos\theta \tag{70}$$

The survival of this term has important consequences, as we shall shortly discuss.

- the scaling behavior of the residual O(3) non-linear sigma model that describes long-wavelength fluctuations of the channel magnetization,
- the residual topological defects of the channel magnetization field $\hat{n}(x)$. These defects carry gauge charge.

D. The non-linear sigma model

Once the Anderson-Higgs effect takes place, the residual long-wavelength behavior is described by an O(3) nonlinear sigma model (NLσM) with bare coupling constant $\tilde{g} = g/N$. In the large N limit, the small size of $\tilde{g}$ means that the channel magnetization is always present in the ground-state. However, we shall now consider the effects of scaling at finite N, considering the stiffness $\tilde{g}$ to be finite. The O(M) σ-model has been extensively studied in the past. [31,33,34] The coupling constant g has dimension $\dim[g] = 2-(d+1) = 1-d$ and its renormalization flow at weak coupling is determined by the beta function,

$$\beta(g) = \frac{dg}{d\ell} = (1-d)g + \frac{(M-2)\Omega_{d+1}}{(2\pi)^{d+1}} g^2, \tag{71}$$

where $d\ell = -\log D$ and Ω_{d+1} is the solid angle in $d+1$ dimensions. Above the lower critical dimension $d > 1$, the scaling flow develops a new fixed point corresponding to the quantum critical point between a disordered $g = \infty$ and ordered $g \to 0$ phase. The critical fixed point is accessible analytically either in the limit of $d = 1+\epsilon$ or $M \to \infty$. In our case $d = 2, 3$ and $M = 3$.

At the lower critical dimension $d = 1$, any value of the coupling constant g renormalizes to infinity $g \to \infty$ corresponding to a quantum disordered (paramagnet) phase. One-dimensional two-channel Kondo lattices have been studied in the past using bosonization [35] as well as density-matrix renormalization group [36] and while there is evidence for non-Fermi liquid phases and channel-antiferromagentic correlations, no channel-ferromagnetic state was reported.

For $d > 1$, a small bare coupling renormalizes to zero $g \to 0$, corresponding to the ordered phase. However, for $g > g_c$, again the system flows to the disordered phase $g \to \infty$. For $g < g_c$ and $d > 1$, the NLσM describes the spontaneous breaking of the channel symmetry and the consequent two Goldstone modes. They have linear dispersion as the channel magnetization order parameter does not commute with the Hamiltonian, in agreement with previous work. [20] The third Goldstone mode, associated with the hybridization phase $e^{i\varphi}$ is Higgsed as we discussed before.

E. Topological Defects

The topology of the emergent channel magnetization admits skyrmions in two dimensions and hedgehog defects in three dimensions ($\pi_2[O(3)] = \mathbb{Z}$). Just as the Anderson-Higgs effect in a superconductor causes a vortex to bind a magnetic flux quantum in a superconductor, here, the Berry phase of the skyrmion or hedgehog will bind a flux quantum in two dimensions, or a monopole in three dimensions. Both gapped, and ungapped electrons feel this field as a *physical* vortex or monopole field.

For gapless c_2 electrons this is simply a consequence of the fact that they experience the gauge potential $A_\mu^{\rm ext} - \frac{1}{2}\Omega_\mu$. We note that the curl of the Berry phase term is related to the curvature of the $\hat{n}$ field via the Mermin-Ho relation,

$$\partial_\mu \Omega_\nu^z - \partial_\nu \Omega_\mu^z = \hat{n} \cdot (\partial_\mu \hat{n} \times \partial_\nu \hat{n}). \tag{72}$$

The quantity

$$\frac{1}{2}\int dS_i \epsilon_{ijk} \hat{n} \cdot (\partial_j \hat{n} \times \partial_k \hat{n}) = 4\pi \mathcal{Q} \tag{73}$$

measures the total solid angle swept out by the order parameter across surface S, which is equal to 4π times the (integer) number $\mathcal{Q}$ of defects, hedgehogs (3D) or skyrmions (2D), enclosed by the surface S.

Thus even in absence of an external field, the phase accumulated by the c_2 electrons around static defect is

$$\frac{e}{\hbar}\Phi_{c2} = \frac{1}{2}\int d\vec{S} \cdot \nabla \times \vec{\Omega}^z = 2\pi \mathcal{Q} \tag{74}$$

or $\Phi_{c2} = \mathcal{Q}\frac{h}{e}$. Any transport experiment involves the gapless c_2 electrons and can potentially detect this experienced phase.

To understand how this works for the gapped electrons, note that the Higgs mass terms enforce the constraint

$$\Omega_\mu^z = 2(A_\mu^{ext} - A_\mu^f) \tag{75}$$

The connection between the Berry curvature and the vector potential fields is closely analogous to a superconductor. In both cases, the energetic requirement that supercurrents vanish at large distances gives rise to the binding of flux to the defect.

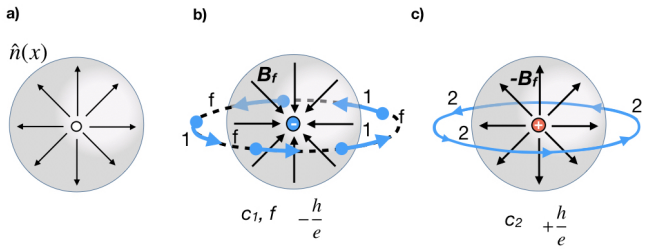

FIG. 5: (a) Hedgehog defect of the $\hat{n}$ field in 3 dimensions. (b) Hybridized conduction and f-fermions in channel 1 see the defect as a negative monopole (c) unhybridized c-fermions see the defect as a positive monopole.

Using the Mermin-Ho relation (72) and the Higgs constraint (75), it follows that

$$4\pi \mathcal{Q} = \int dS_i \epsilon_{ijk} \partial_j \Omega_k$$

$$= 2 \int d\vec{S} \cdot \vec{\nabla} \times (\vec{A}^{ext} - \vec{A}^f) \tag{76}$$

or

$$\int d\vec{S} \cdot \vec{\nabla} \times (\vec{A}^{ext} - \vec{A}^f) = \int d\vec{S} \cdot (\vec{B}^{ext} - \vec{B}^f) = 2\pi Q. \tag{77}$$

This tells us that the topological defect must bind a flux quantum of the difference field, much in the way a superconducting vortex binds a magnetic flux quantum. In the case of a skyrmion, this corresponds to a magnetic flux quantum of the difference field. (In practice the larger energy cost of a magnetic field will likely mean the bound quantum is largely in the f-field). However, for a hedgehog defect in three dimensions the strict absence of electromagnetic monopoles guarantees that $\int d\vec{S} \cdot \vec{B}^{ext} = \int d^3x \vec{\nabla} \cdot \vec{B}^{ext} = 0$. In this case we can eliminate the electromagnetic component of the surface integral. This means that the total f-flux bound to a $\mathcal{Q}$ hedgehog is

$$\frac{e}{\hbar} \Phi_f = \int d\vec{S} \cdot \vec{\nabla} \times \vec{A}^f = -2\pi \mathcal{Q} \tag{78}$$

where we have restored the $e/\hbar$ to the definition of flux. Thus

$$\Phi_f = -\mathcal{Q} \frac{h}{e} \tag{79}$$

so that each hedgehog or skyrmion carries unit magnetic flux of the f-field, forming a vison monopole.

Remarkably, when we work it through, we find that the Berry phase field experienced by the conduction electrons means that they also feel the vison field. In fact, the f-electrons and the conduction electrons they hybridize with in channel 1 experience the vector potential $\vec{A}^f$, whereas the gapless channel 2 fermions experience a vector potential $-\vec{A}^f$, as if the two channels have acquired an opposite charge. To see this, let us first set the electromagnetic potential to zero $A_\mu^{ext} = 0$. The resulting vector potential of the conduction electrons is then

$$\mathbf{A}_a = -\frac{1}{2} \Omega_a^z \tau_3 \rightarrow A_f \tau_3 \equiv \begin{cases} A_f & c_1 \\ -A_f & c_2 \end{cases} \tag{80}$$

In this way all electrons feel the monopole, in such a way that the hybridized and unhybridized electrons experience an equal and opposite monopole vector potential. One of the interesting effects of the monopole field will be to produce bound-states in the gap. Within the ordered phases, this opens up the interesting possibility that topological configurations of the order parameter can be detected by purely electronic transport studies.

F. Phase diagram

In the channel ferromagnetic phase the skyrmions are gapped, [37] with an energy given by $4\pi \mathcal{Q} g^{-1}$. Therefore, at low-enough temperature, the action (65) reduces to a separate sum of a $U(1)$ field, as in a single-channel Kondo insulator, Eq. (69), and the NLσM term describing the fluctuations of the Goldstone modes. In this phase, we have the phase-locking $A^f = A^{\rm ext}$ and as discussed above, a large total Fermi surface (albeit only the Fermi surface of one conduction band is expanded).

Close to a quantum critical point into another ordered phase, e.g, magnetism, the Kondo temperature is suppressed to zero [38,39] and the Higgs mode also becomes soft. The correct description then, includes this soft term and is beyond the treatment adapted here.

However, within the $\langle V^2 \rangle \neq 0$ regime, we expect a separate quantum critical point defined by the NLσM physics at $g = g_c$. For $g_0 > g_c$ within perturbative RG, $g \rightarrow \infty$ and the ground state is disordered. The nature of the groundstate in this phase is quite interesting and we can gain a guide to it using the physics of the $O(M)$ NLσM. In the large M limit of this model, we know that the z-spinons (long-wavelength fluctuations of channel magnetization $\vec{n}$) are gapped. [34] However, the topological defects proliferate and condense. [31,40,41] This process will eliminate the phase-locking between the electromagnetic and f-fermion gauge fields, and the resulting electronic Fermi surface will become small again. This is schematically shown in Fig. 6(b). Were such a phase transition to occur in a real material, we might expect it to exhibit a jump in the FS. In contrast to a magnetic transition, the magnetic susceptibility is expected to remain finite at this transition.

Besides having a small Fermi surface, the nature of the ground state in the quantum disordered phase remains unclear. Assuming that the resulting phase is a Fermi liquid, this small FS appears to violate Oshikawa's theorem. [23] A trivial resolution to this paradox might be that the adiabatic assumption of the flux-threading is violated due to the gapless nature of the spin-liquid. However, as discussed before, the hybridization is non-zero in the quantum disordered phase and the f-spinons are likely to remain gapped, as in the channel ferromagnet phase. Therefore, a better resolution to this paradox is that the ground state has topological order (i.e. degeneracy on a torus). [42] In that case, after an adiabatic threading of a flux through the torus holes the system need not be back to the same ground state. Based on this, we conjecture that the quantum disordered phase of a two-channel Kondo lattice may have topological order, realizing a fractionalized Fermi liquid (FL*).

IV. CONCLUSION AND OUTLOOK

We have shown that in the large-N limit the ground state develops a spontaneously broken channel symmetry, most naturally understood in terms of order fractionalization: a process which involves the separation of the composite spin-fermion bound states into a fermionic resonance and a half-integer order parameter, manifested

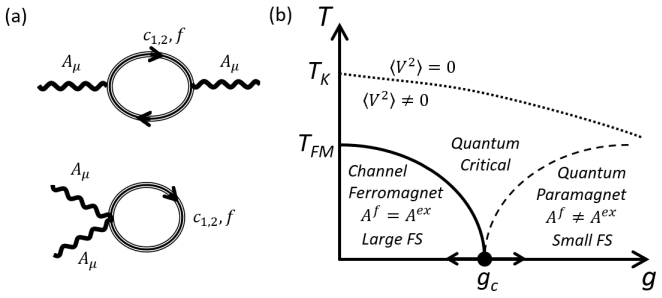

FIG. 6: (a) The basic diagrams (paramagnetic and diamagnetic contributions) involved in integrating out the fermions to one loop. (b) The phase diagram for $d = 3$. The same phase diagram applies to $d = 2$, except that $T_{FM} \to 0$. The sold lines are second order phase transition and the dashed line is a crossover. In the channel ferromagnet $g \to 0$. In this phase internal and external gauge fields are phase-locked $A^f = A^{\rm ext}$, resulting in a large Fermi Surface (FS). For $g > g_c$ the system is in the quantum disordered phase, where $A^f \neq A^{\rm ext}$ and the Fermi surface is smaller.

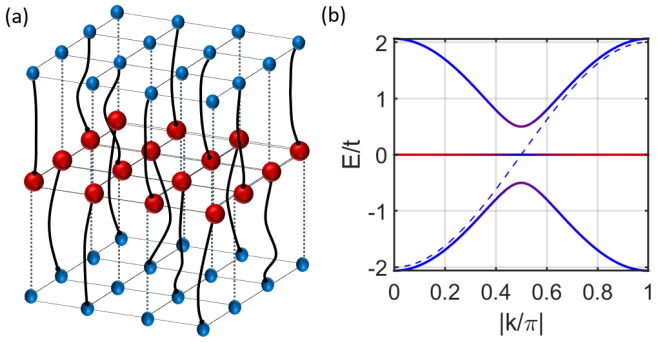

FIG. 7: (a) Channel antiferromagnetic state: the hybridization between the local moments (red) alternates between the two channels at every other site. (b) Schematic representation of the band structure of the staggered hybridization state.

in the long-time behavior of the electronic self-energy.

Our analysis of collective soft modes shows that the effective action is composed of a non-linear sigma term describing symmetry breaking and the Goldstone modes, and a Kondo-Higgs term which causes the phase-locking of internal and external gauge fields, and the expansion of the Fermi surface. These two terms become intertwined in the presence of topological defects, which behave as monopoles with a $U(1)$ gauge charge which locally destroys the phase locking between the fields. This allows us to predict that when these defects proliferate in the quantum disordered phase of the two-channel Kondo lattice, the Fermi surface jumps from large to small, with experimental consequences.

These arguments lead us to expect that in addition to the channel ferromagnetic phase, the higher-dimensional (two or three-dimensional) two-channel Kondo lattices, have a quantum disordered phase, possibly with topological order. Although this phase has not yet been seen in experiments using pressure or magnetic field as the tuning parameter, it may be revealed by using these tuning parameters in combination to allow a more extensive exploration of the phase diagram.

Our results suggest a number of interesting directions for future work. For example, a more complete analysis of the particle-hole symmetric two-channel Kondo soft modes will need to take into account the full $SP(4) \sim SO(5)$ symmetry of the problem, [4] a symmetry that allows the rotation between channel magnets and composite paired (odd-frequency) superconducting ground-states. At the impurity level (or in quantum disordered phases in larger d), the order parameter strongly fluctuates, exploring the full symmetry group. This appears to be responsible for capturing the residual entropy of the two-channel Kondo impurity. Moreover, the term $C^\dagger A^z_\tau \tau^z C$ in the Lagrangian (57) can be interpreted as a Berry phase for the order parameter $\vec{n}$. Within one-loop and at half-filling, the coefficient of this term $\langle C^\dagger \tau^z C \rangle$ is zero. However, $C^\dagger \tau^z C$ does not commute with the Hamiltonian and the Berry phase might have important effects beyond one-loop.

Further work is also required to understand the ground state and excitations of the quantum-disordered phase of the two channel Kondo lattice and possible topological order that may develop in this phase. In particularly, the relationship of this phase to deconfined criticality will require studying defect proliferation.

ACKNOWLEDGMENTS

It is a pleasure to thank Premala Chandra, Indranil Paul, Elio König, Weida Wu, Senthil Todadri, Philipp Gegenwart and Achim Rosch for fruitful discussions. P. C. and A. W. were supported by the National Science Foundation grant DMR-1830707. Y. K. was supported by a Rutgers University Materials Theory postdoctoral fellowhsip.

APPENDICES

The appendices contain additional proofs and details that are used in the paper. The uniform mean-field solution is compared to an alternative staggered solution in Appendix A. In Appendix B we describe a continuum model for the Kondo lattice that is used in field theory calculations. Appendix C contains a derivation of the effective action, which is a central point of the paper.

Appendix A: Staggered Hybridization Solution

In this section, we compare the half-Kondo-insulator solution with an alternative channel symmetry breaking mean-field state, for which the hybridization is staggered

in channel space. The corresponding mean field configuration is

$$\lambda_j = 0, \quad V_j = V, \qquad \varphi_j = \varphi, \tag{A1}$$

$$\phi_j = 0, \qquad \theta_j = \frac{\pi}{4}\left[1 - e^{i\pi(j_1+j_2)}\right]. \tag{A2}$$

The hybridization term can be further simplified by choosing the gauge with

$$\begin{pmatrix} \tilde{c}_{\vec{k}1\alpha} \\ \tilde{c}_{\vec{k}1\alpha} \end{pmatrix} = \frac{1}{\sqrt{2}} \begin{pmatrix} 1 & 1 \\ 1 & -1 \end{pmatrix} \begin{pmatrix} c_{\vec{k}1\alpha} \\ c_{\vec{k}2\alpha} \end{pmatrix}, \tilde{f}_{\vec{k}\alpha} = e^{i\phi} f_{\vec{k}\alpha}. \tag{A3}$$

The band energies are each doubly degenerate with values

$$E^{1,2} = 0, \; E^{3,4}_{\vec{k}} = -\sqrt{\epsilon^2_{\vec{k}} + V^2}, \; E^{5,6}_{\vec{k}} = \sqrt{\epsilon^2_{\vec{k}} + V^2}. \tag{A4}$$

The free energy per site per particle is then given by

$$\frac{F}{N\mathcal{N}_s} = -4T \int\limits_{\frac{1}{2}\text{B.Z.}} \frac{\mathrm{d}^2k}{(2\pi)^2} \log\left[2\cosh\left(\frac{\sqrt{\epsilon^2_{\vec{k}} + V^2}}{2T}\right)\right] - 2T\log(2) + \frac{V^2}{J}, \tag{A5}$$

and the hybridization strength is determined self-consistently from

$$\frac{1}{N\mathcal{N}_s}\frac{\delta F}{\delta V^2} = \frac{1}{J} - \int\limits_{\frac{1}{2}\text{B.Z.}} \frac{d^2k}{(2\pi)^2} \frac{\tanh\left(\frac{\sqrt{\epsilon^2_{\vec{k}}+V^2}}{2T}\right)}{\sqrt{\epsilon^2_{\vec{k}} + V^2}} = 0.$$

Using a constant density of states $\rho = (8t)^{-1}$, we can estimate the hybridization strength at zero temperature to be

$$V^{-1} = 2\rho \sinh\left(\frac{1}{\rho_0 J}\right). \tag{A6}$$

In figure 4(b), the free energy is plotted for varying hybridization strength for both uniform and staggered hybridization. As stated before, the uniform solution has lower energy and is therefore a better candidate for the ground state.

Appendix B: A Continuum Kondo Insulator

Kondo lattices in the large-N limit are usually studied on tight-binding models. For the derivation of the NLσM and the study of the skyrmion spectrum it is much easier to use an approximate low-energy description of the Kondo lattice which has continuous translational and rotational symmetry. In other words, we consider the momentum-space Hamiltonian

$$H = \sum_k \begin{pmatrix} c^\dagger_k & f^\dagger_k \end{pmatrix} \begin{pmatrix} \epsilon^c_k & V \\ V & \epsilon^f_k \end{pmatrix} \begin{pmatrix} c_k \\ f_k \end{pmatrix} + N\mathcal{N}_s \left(\frac{V^2}{J_K} - \lambda q_f\right) \tag{B1}$$

where

$$\epsilon^c_k = \frac{k^2}{2m_c} - \mu, \quad \text{and} \quad \epsilon^f_k = -\frac{k^2}{2m_f} + \lambda, \tag{B2}$$

and $q_f = Q_f/N$. Eq. (B1) describes the low-energy Hamiltonian of a Kondo-Heisenberg system. The dispersion of f-electrons arises due to antiferromagnetic Heisenberg interactions between the spins. In order to have a Kondo insulator we have assumed opposite sign of mass for conduction and f-electrons. Due to lack of particle-hole symmetry, it is not clear whether a continuum version of a Kondo insulator exists. The main challenge is to show that the conditions of having a spectral gap and the constraint $n_f = Q_f$ can be simultaneously realized in this system. To be specific, we limit our discussion to $d = 2$ spatial dimensions.

The Hamiltonian (B1) can be diagonalized using an O(2) rotation

$$\begin{pmatrix} c_k \\ f_k \end{pmatrix} = \begin{pmatrix} \cos\alpha_k & -\sin\alpha_k \\ \sin\alpha_k & \cos\alpha_k \end{pmatrix} \begin{pmatrix} l_k \\ h_k \end{pmatrix} \tag{B3}$$

where

$$\tan 2\alpha_k = \frac{2V}{\epsilon^c_k - \epsilon^f_k} \tag{B4}$$

leading to the energy eigenvalues

$$E^{l/h}_k = \frac{\epsilon^c_k + \epsilon^f_k}{2} \pm \sqrt{\left(\frac{\epsilon^c_k - \epsilon^f_k}{2}\right)^2 + V^2}. \tag{B5}$$

Due to π-periodicity of the $\tan 2\alpha_k$, we are free to choose either the period $2\alpha_k \in (0, \pi)$ or $2\alpha_k \in (-\pi/2, \pi/2)$. We choose the former interval, because the angle evolves more continuously in the Brillouin zone. Therefore,

$$\sin 2\alpha_k = \frac{2V}{E^l_k - E^h_k}, \qquad \cos 2\alpha_k = \frac{\epsilon^c_k - \epsilon^f_k}{E^l_k - E^h_k}. \tag{B6}$$

For a Kondo insulator, the E^h band is fully occupied, while the E^l band is empty, so that the ground-state free energy is

$$\frac{F}{N\mathcal{N}_s} = \frac{V^2}{J_K} + \int \frac{d^2k}{(2\pi)^2} E^h_k - \lambda q_f \tag{B7}$$

Varying F with respect to V^2 gives the mean-field equation

$$\frac{1}{J_K} = \int \frac{d^2k}{(2\pi)^2} \frac{1}{\sqrt{(\epsilon^c_k - \epsilon^f_k)^2 + 4V^2}} \tag{B8}$$

while varying it with respect to λ enforces the constraint. For the inverted f-electron band, it is more convenient to apply the constraint to the f-hole occupation

$$\tilde{q}_f \equiv 1 - q_f = \frac{1}{L}\sum_k \left\langle f_k f^\dagger_k \right\rangle. \tag{B9}$$

In the absence of hybridization in $d = 2$, the f-hole density is

$$\tilde{q}_f = \int \frac{d^2k}{(2\pi)^2} f(-\epsilon_k^f) \xrightarrow{T=0} \frac{m_f}{2\pi} |\lambda_0| \tag{B10}$$

Similarly, the density of electrons (per spin) is given by

$$q_c = \frac{m_c}{2\pi}\mu. \tag{B11}$$

In presence of hybridization and temperature much lower than the gap, only the E^h band is occupied. Therefore, the density of f-holes and c-electrons is the same and is given by

$$\tilde{q}_f = q_c = \int \frac{d^dk}{(2\pi)^d} \sin^2 \alpha_k = \\ = \frac{1}{2}\int \frac{d^dk}{(2\pi)^d}\left[1 - \frac{\epsilon_k^c - \epsilon_k^f}{\sqrt{(\epsilon_k^c - \epsilon_k^f)^2 + 4V^2}}\right] \tag{B12}$$

In the continuum limit, eqs. (B8) and (B12) become

$$\frac{1}{J_K} \approx \nu \sinh^{-1}\left[\frac{\Lambda^2}{8\pi\nu V}\left(\eta + \sqrt{\eta^2+1}\right)\right] \tag{B13}$$

$$\tilde{q}_f \approx \nu V \sqrt{\eta^2+1} \tag{B14}$$

where $\nu \equiv [2\pi/m_c + 2\pi/m_f]^{-1}$ is an average density of states of the c and f bands, Λ is the high-energy momentum cut-off and $\eta \equiv (\mu+\lambda)/2V$ is a short-hand notation. The first equation suggests defining

$$T_K \equiv \frac{\Lambda^2}{8\pi\nu \sinh\left(\frac{1}{\nu J_K}\right)}. \tag{B15}$$

In terms of T_K, eqs. (B13) and (B14) can be solved for

$$V = \sqrt{2DT_K - T_K^2} \quad \text{and} \quad \lambda \approx 2D - \mu - 2T_K, \tag{B16}$$

where $D \equiv \tilde{q}_f/\nu \gg T_K$ is an emergent energy scale, which plays the role of an effective bandwidth and we have expanded the expression for λ to leading order in T_K/D. In the following, it is convenient to introduce two dimensionless parameters:

$$t_K \equiv T_K/D, \qquad r_m \equiv m_c/m_f \tag{B17}$$

in terms of which

$$V/D \approx (\eta^2+1)^{-1/2} \approx \sqrt{2t_K}. \tag{B18}$$

For a physical realization of a Kondo insulator we expect $t_K \ll 1$ and $r_m \ll 1$ and all following expressions assume this limit. The presence of a Kondo insulator, requires having the chemical potential inside the gap. In particular, the minimum of the upper band, E^l, has to be above zero energy and the maximum of the lower band, E^h, has to be below zero energy. This constraints the chemical potential to be in the region

$$2 - 2t_K - \sqrt{8r_m t_K} \lessapprox \mu/D \lessapprox 2 - 2t_K, \tag{B19}$$

for $t_K \gtrapprox 2r_m$ and

$$2 - 2t_K - \sqrt{8r_m t_K} \lessapprox \mu/D \lessapprox 2 - 2t_K + \sqrt{8r_m t_K} \tag{B20}$$

for $t_K \lessapprox 2r_m$. The gap closes in either case of $r_m \to 0$ or $t_K \to 0$. However, the order of limits matters and the indirect gap is given by $D\sqrt{8r_m t_K}$ and $2D\sqrt{8r_m t_K}$ for $t_K > 2r_m$ and $t_K < 2r_m$, respectively.

An example of a band structure of such a continuum Kondo insulator is depicted in Fig. (8).

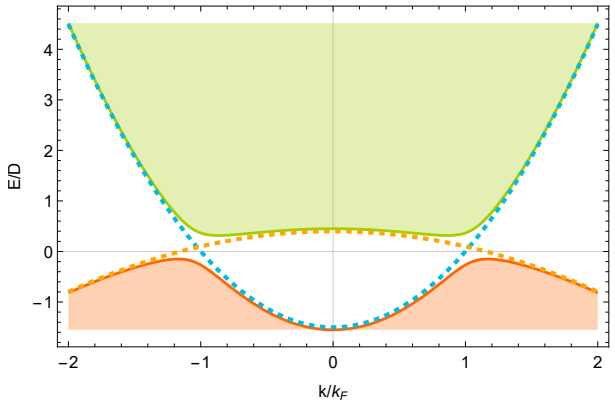

FIG. 8: An example of a continuum Kondo insulator in 2D. The model parameters are $m_f/m_c = 5$, $\mu/D = 1.5$ and $T_K/D = 0.05$. The dashed green line corresponds to the c-electrons, while the f-electrons are depicted by the dashed orange line. After these two bands hybridize, we obtain a lower band, E^h (solid orange line), and an upper band, E^l (solid green line).

Appendix C: Derivation of the Effective action

We start from the Lagrangian (57). Integrating out the fermions, the free energy is

$$F(A) = -NT\mathrm{Tr}\log[-\mathcal{G}^{-1}(A)] + F_b(A), \tag{C1}$$

where

$$-\mathcal{G}^{-1}(A) = \left(\begin{array}{cc|c} & & V \\ & -\mathfrak{g}_C^{-1} & 0 \\ \hline V & 0 & -g_f^{-1} \end{array}\right), \tag{C2}$$

and

$$F_b[A] = i(A_\tau^{\mathrm{ext}} n_c + A_\tau^f Q)\mathcal{N}_s, \tag{C3}$$

is the background free energy due to the coupling of the potentials to the background conduction and f-electron charge. These terms ensure that when we expand the

effective action in the applied fields, terms linear in the coupling identically vanish. We can write

$$\begin{aligned}\Delta F(A) &\equiv F(A) - F(A=0) \\ &= -NT\mathrm{Tr}\log\left\{1-\mathcal{G}\mathcal{W}\right\} + F_b(A) \end{aligned} \tag{C4}$$

where $\mathcal{G} \equiv \mathcal{G}(A=0)$ and $\mathcal{W}$ are given by

$$\mathcal{W} = \left(\begin{array}{cc|c} & & 0 \\ & \mathbb{W} & 0 \\ \hline 0 & 0 & w^f \end{array}\right), \quad \mathcal{G} = \left(\begin{array}{cc|c} & & G_{1f} \\ & \mathbb{G}_C & 0 \\ \hline G_{1f} & 0 & G_f \end{array}\right), \tag{C5}$$

where in the momentum-frequency domain the Green's functions are given by

$$\mathbb{G}_{\mathbb{C}} = \mathrm{diag}\left[G_1 = \frac{z-\varepsilon_k^f}{\left(z-E_k^l\right)\left(z-E_k^h\right)}, g_2 = \frac{1}{z-e_k^c}\right] \tag{C6}$$

$$G_{1f} = \frac{V}{\left(z-E_k^l\right)\left(z-E_k^h\right)} \tag{C7}$$

$$G_f = \frac{z-\varepsilon_k^c}{\left(z-E_k^l\right)\left(z-E_k^h\right)}. \tag{C8}$$

In order to take the trace over channel indices, it is convenient to expand $\mathbb{G}_{\mathbb{C}}$ in terms of Pauli matrices in channel space $\mathbb{G}_{\mathbb{C}} = G^0\tau^0 + G^3\tau^3$. Additionally, we have defined the short-hand symbols

$$\mathbb{W} = i\mathbb{A}_\tau - \frac{1}{2m_c}\sum_{\nu=1}^{d}[i\partial_\nu\mathbb{A}_\nu + 2i\mathbb{A}_\nu\partial_\nu - \mathbb{A}_\nu\mathbb{A}_\nu]$$

$$w^f = iA_\tau^f + \frac{1}{2m_f}\sum_{\nu=1}^{d}[i\partial_\nu A_\nu^f + 2iA_\nu^f\partial_\nu - A_\nu^f A_\nu^f], \tag{C9}$$

where, following section (III A), the conduction electron vector potential contains a Berry phase and an electromagnetic term, given by $\mathbb{A}_\mu = A_\mu^a\tau_a = \frac{1}{2}\Omega_\mu^a\tau_a - \tau_0 A_\mu^{ext}$. Defining

$$\mathcal{X} = \mathcal{G}\mathcal{W} = \left(\begin{array}{c|c} \mathbb{G}_C\mathbb{W} & \begin{array}{c} G_{1f}w^f \\ 0 \end{array} \\ \hline \begin{array}{cc} G_{1f}\left[\mathbb{W}\right]_{11} & 0 \end{array} & G_f w^f \end{array}\right) \tag{C10}$$

and expanding the log

$$-\log(1-\mathcal{X}) \approx \mathcal{X} + \mathcal{X}^2/2, \tag{C11}$$

to $O(A^2)$ leads to

$$\frac{\Delta F}{NT} = \mathrm{Tr}\Big\{\mathbb{G}_c\mathbb{Q} + G_f q_f + \frac{1}{2}(\mathbb{G}_C\mathbb{Q})^2 + \frac{1}{2}(G_f q_f)^2 + G_{1f}Q_{11}G_{1f}q_f\Big\} - F_b[A] \tag{C12}$$

$$\begin{aligned} &= \mathrm{Tr}\Big\{\frac{1}{2m_c}\mathbb{G}_C\mathbb{A}_\nu\mathbb{A}_\nu + \frac{1}{2m_f}G_f A_\nu^f A_\nu^f - \frac{1}{2}\mathbb{G}_C\mathbb{A}_\tau\mathbb{G}_C\mathbb{A}_\tau - \frac{1}{8m_c^2}\mathbb{G}_C\Big(\cancel{\partial_\nu\mathbb{A}_\nu} + 2\mathbb{A}_\nu\partial_\nu\Big)\mathbb{G}_C\Big(\cancel{\partial_{\nu'}\mathbb{A}_{\nu'}} + 2\mathbb{A}_{\nu'}\partial_{\nu'}\Big) \\ &\quad -\frac{1}{2}A_\tau^f G_f A_\tau^f G_f - \frac{1}{8m_f^2}(\cancel{\partial_\nu A_\nu^f} + 2A_\nu^f\partial_\nu)G_f(\cancel{\partial_{\nu'}A_{\nu'}^f} + 2A_{\nu'}^f\partial_{\nu'})G_f - G_{1f}A_\tau^{C,11}G_{1f}A_\tau^f \\ &\quad \frac{G_{1f}}{4m_c m_f}(\cancel{\partial_\nu A_\nu^{C,11}} + 2A_\nu^{C,11}\partial_\nu)G_{1f}(\cancel{\partial_{\nu'}A_{\nu'}^f} + 2A_{\nu'}^f\partial_{\nu'})\Big\}. \end{aligned} \tag{C13}$$

Here, the trace is taken over all space/time and channel variables. The terms linear in the applied fields vanish, because the net charge densities and currents are identically zero in the ground-state, while the terms containing odd numbers of time or space derivatives also vanish, as they are odd under time-reversal or spatial inversion. We have also omitted higher derivatives of A (see below). Lastly, anticipating the long-wavelength limit ($\vec{q} \to 0$), we have neglected the terms that contain the divergence of the gauge fields.

1. Terms quadratic in A_τ

In momentum space, the quadratic terms have the generic form

$$\frac{1}{\beta}\sum_{i\omega_n, i\nu_r}\int\frac{\mathrm{d}^2k\mathrm{d}^2q}{(2\pi)^4}G(i\omega_n,\vec{k})A(i\nu_r,\vec{q}) \\ G(i\omega_n + i\nu_r, \vec{k}+\vec{q})A(-i\nu_r,-\vec{q}). \tag{C14}$$

Here, we assume a slow variation of the gauge potentials in space/time and only keep the lowest order in $i\nu_r$ and $\vec{q}$ in the Green's functions. Terms quadratic in gauge

potential and containing only the time-components are

$$\frac{\Delta F_{temporal}}{NT} = \Lambda^{00}\int d\bar{x}_\mu \sum_{a=0}^{3}[A^a_\tau(\bar{x}_\mu)]^2 + \Lambda^{33}\int d\bar{x}_\mu\Big\{\sum_{a=0,3}-\sum_{a=1,2}\Big\}[A^a_\tau(\bar{x}_\mu)]^2 + 4\Lambda^{03}\int d\bar{x}_\mu A^0_\tau(\bar{x}_\mu)A^3_\tau(\bar{x}_\mu) + \frac{\Lambda^{ff}}{2}\int d\bar{x}_\mu[A^f_\tau(\bar{x}_\mu)]^2 + \Lambda^{1f,1f}\int d\bar{x}_\mu[A^0_\tau(\bar{x}_\mu)+A^3_\tau(\bar{x}_\mu)]A^f_\tau(\bar{x}_\mu) \quad \text{(C15)}$$

where we have defined

$$\Lambda^{ab} \equiv -\lim_{i\nu_r\to 0,\vec{q}\to 0}\frac{1}{\beta}\sum_{i\omega_n}\int\frac{\mathrm{d}^2k}{(2\pi)^2} G^a(i\omega_n,\vec{k})G^b(i\omega_n+i\nu_r,\vec{k}+\vec{q}), \quad \text{(C16)}$$

where the G^a are the components in the Pauli-matrix decomposition $\mathbb{G}_\mathbb{C} = G^0\tau^0 + G^3\tau^3$ of conduction electron propagator. The order of limits as indicated is crucial for extracting gauge-invariant results. These terms are of the form

$$(\Lambda^{00}+\Lambda^{33})[(A^0_\tau)^2+(A^3_\tau)^2] + (\Lambda^{00}-\Lambda^{33})[(A^1_\tau)^2+(A^2_\tau)^2] + 4\Lambda^{03}A^0_\tau A^3_\tau + \frac{1}{2}\Lambda^{ff}(A^f_\tau)^2 + \Lambda^{1f,1f}[A^0_\tau+A^3_\tau]A^f_\tau. \quad \text{(C17)}$$

We can compute the coefficients using mean-field Green's functions. We find

$$\Lambda^{00}+\Lambda^{33} = 2\Lambda^{03} = \Lambda^{ff} = \frac{1}{2}\Lambda^{1f,1f}. \quad \text{(C18)}$$

as demanded by the gauge invariance of the original Hamiltonian. Various terms can be combined and the effective Lagrangian contains

$$\frac{\mathcal{L}_{temporal}}{N} = 2\Gamma(A^0_\tau + A^3_\tau - A^f_\tau)^2 + \frac{1}{2g}[(A^1_\tau)^2+(A^2_\tau)^2]. \quad \text{(C19)}$$

Here the definition of parameters is deliberate as we recognize the Higgs term from section III B. In appendix C 3 we will identify the second term as the temporal part of the NLσM.

We can calculate the coefficients explicitly in the limit $T \ll T_K$ for the continuum model discussed in the previous section.

$$2\Gamma = \Lambda^{00}+\Lambda^{33} = -\lim_{i\nu_r\to 0,\vec{q}\to 0}\frac{1}{2\beta}\sum_{i\omega_n}\int\frac{\mathrm{d}^2k}{(2\pi)^2}\Big[G_1(i\omega_n,\vec{k})G_1(i\omega_n+i\nu_r,\vec{k}+\vec{q}) + g_2(i\omega_n,\vec{k})g_2(i\omega_n+i\nu_r,\vec{k}+\vec{q})\Big]$$
$$\frac{1}{2g} = \Lambda^{00}-\Lambda^{33} = -\lim_{i\nu_r\to 0,\vec{q}\to 0}\frac{1}{2\beta}\sum_{i\omega_n}\int\frac{\mathrm{d}^2k}{(2\pi)^2}\Big[G_1(i\omega_n,\vec{k})g_2(i\omega_n+i\nu_r,\vec{k}+\vec{q}) + g_2(i\omega_n,\vec{k})G_1(i\omega_n+i\nu_r,\vec{k}+\vec{q})\Big]$$

Taking the Matsubara sum we obtain

$$2\Gamma = \sum_k \frac{V^2}{\Big[(\epsilon^c_k-\epsilon^f_k)^2+4V^2\Big]^{3/2}},$$
$$\frac{1}{2g} = \sum_k\left[\frac{\sin^2\alpha_k f(-\epsilon_k)}{\epsilon_k-E_h} - \frac{\cos^2\alpha_k f(\epsilon_k)}{\epsilon_k-E_l}\right], \quad \text{(C20)}$$

where we have set the Fermi functions to $f(E^h)=1$ and $f(E^l)=0$, because we have a Kondo insulator. Carrying out the momentum integrals in two spatial dimensions we obtain in terms of the variables of appendix B

$$2\Gamma = \frac{\nu}{4}\left[1+\frac{\eta}{\sqrt{1+\eta^2}}\right],$$
$$\frac{1}{2g} = \nu\left[\frac{1}{2}-\eta^2+\eta\sqrt{1+\eta^2}\right] + \frac{\nu}{2}\frac{(\lambda+r_m\mu)^2}{V^2}. \quad \text{(C21)}$$

These results can be simplified in the regime where $t_K = T_K/D$ and $r_m = m_c/|m_f|$ are both small and consequently $\eta \sim D/V \gg 1$ and $\mu/D \approx 2$:

$$2\Gamma \approx \frac{\nu}{2} \quad \text{(C22)}$$
$$\frac{1}{2g} \approx \nu\mathcal{Z}, \qquad \mathcal{Z} \equiv \left[1+t_K(1+r_m/t_K)^2\right]. \quad \text{(C23)}$$

2. Terms quadratic in A_x

Terms quadratic in gauge potential and containing only the spatial components are

$$\begin{aligned}\frac{\Delta F_{spatial}}{NT} &= \Lambda^{00}_{\nu\nu'}\int d\bar{x}_\mu \sum_{a=0}^{3} A^a_\nu(\bar{x}_\mu)A^a_{\nu'}(\bar{x}_\mu)\\ &+\Lambda^{33}_{\nu\nu'}\int d\bar{x}_\mu\Big\{\sum_{a=0,3}-\sum_{a=1,2}\Big\}A^a_\nu(\bar{x}_\mu)A^a_{\nu'}(\bar{x}_\mu)\\ &+4\Lambda^{03}_{\nu\nu'}\int d\bar{x}_\mu A^0_\nu(\bar{x}_\mu)A^3_{\nu'}(\bar{x}_\mu)\\ &+\frac{\Lambda^{ff}_{\nu\nu'}}{2}\int d\bar{x}_\mu A^f_\nu(\bar{x}_\mu)A^f_{\nu'}(\bar{x}_\mu)\\ &+\Lambda^{1f}_{\nu\nu'}\int d\bar{x}_\mu[A^0_\nu(\bar{x}_\mu)+A^3_\nu(\bar{x}_\mu)]A^f_{\nu'}(\bar{x}_\mu)\end{aligned}$$

where we have defined

$$\begin{aligned}\Lambda^{ab}_{\nu\nu'} \equiv \lim_{i\nu_r\to 0,\vec{q}\to 0}\frac{1}{\beta}\sum_{i\omega_n}\int\frac{\mathrm{d}^2k}{(2\pi)^2}\frac{k_\nu}{m^a}G^a\left(i\omega_n-\frac{i\nu_r}{2},\vec{k}-\frac{\vec{q}}{2}\right)\\ \times\frac{k_{\nu'}}{m^b}G^b\left(i\omega_n+\frac{i\nu_r}{2},\vec{k}+\frac{\vec{q}}{2}\right).\end{aligned}\tag{C24}$$

This will turn out to be diagonal in lower indices $\Lambda^{ab}_{\nu\nu'}\propto\delta_{\nu\nu'}$. The structure of these terms is precisely equal to that of the $\Delta F_{2\tau}$ terms we studied before:

$$\begin{aligned}&(\Lambda^{00}_{\nu\nu}+\Lambda^{33}_{\nu\nu})[(A^0_\nu)^2+(A^3_\nu)^2]+(\Lambda^{00}_{\nu\nu}-\Lambda^{33}_{\nu\nu})[(A^1_\nu)^2+(A^2_\nu)^2]\\ &+4\Lambda^{03}_{\nu\nu}A^0_\nu A^3_\nu+\frac{1}{2}\Lambda^{ff}_{\nu\nu}(A^f_\nu)^2+\Lambda^{1f,1f}_{\nu\nu}[A^0_\nu+A^3_\nu]A^f_\nu,\end{aligned}\tag{C25}$$

but these have to be combined with the diamagnetic terms

$$\begin{aligned}\frac{\Delta F_{diag}}{NT} &= \frac{2}{2m_c}\int d\bar{x}_\mu\Big\{\sum_{a=0}^{3}[A^a_\nu(\bar{x}_\mu)]^2G^0_C(0)\\ &\qquad+2A^0_\nu(\bar{x}_\mu)A^3_\nu(\bar{x}_\mu)G^3_C(0)\Big\}\\ &+\frac{1}{2m_f}\int d\bar{x}_\mu[A^f_\nu(\bar{x}_\mu)]^2G_f(0).\end{aligned}\tag{C26}$$

Computing the coefficients of (C25) we have

$$\begin{aligned}\Lambda^{00}_{\nu\nu}+\Lambda^{33}_{\nu\nu} &= \frac{1}{2\beta}\sum_{n,k}[G_1^2(i\omega_n,k)+g_2^2(i\omega_n,k)](v^c_\nu)^2=-\frac{1}{2\beta}\sum_{nk}G^2_{1f}(i\omega_n,k)v^c_\nu v^f_\nu-\frac{1}{2\beta}\sum_{nk}[G_1(i\omega_n,k)+g_2(i\omega_n,k)]\frac{1}{m_c},\\ \Lambda^{00}_{\nu\nu}-\Lambda^{33}_{\nu\nu} &= \frac{1}{\beta}\sum_{nk}G_1(i\omega_n,k)g_2(i\omega_n,k)(v^c_\nu)^2,\\ 4\Lambda^{03}_{\nu\nu} &= \frac{1}{\beta}\sum_{nk}[G_1^2(i\omega_n,k)-g_2^2(i\omega_n,k)](v^c_\nu)^2=-\frac{1}{\beta}\sum_{nk}G^2_{1f}(i\omega_n,k)v^c_\nu v^f_\nu-\frac{1}{\beta}\sum_{nk}\sum_{nk}[G_1(i\omega_n,k)-g_2(i\omega_n,k)]\frac{1}{m_c},\\ \Lambda^{ff}_{\nu\nu} &= \frac{1}{\beta}\sum_{nk}G_f^2(i\omega_n,k)(v^f_\nu)^2=-\frac{1}{\beta}\sum_{nk}G^2_{1f}(i\omega_n,k)v^c_\nu v^f_\nu+\frac{1}{\beta}\sum_{nk}G_f(i\omega_n,k)\frac{1}{|m_f|},\\ \Lambda^{1f,1f}_{\nu\nu} &= \frac{1}{\beta}\sum_{nk}G^2_{1f}(i\omega_n,k)v^c_\nu v^f_\nu.\end{aligned}$$

Here, $v^c_\nu=k_\nu/m_c$, $v^f_\nu=-k_\nu/|m_f|$ and we have used $\partial_{k_\nu}G_1=G_1^2[v^c_\nu+V^2g_f^2v^f_\nu]$ and $G_{1f}=VG_1g_f$ to bring these terms to a form suitable to add the diamagnetic terms. The latter has the following coefficients:

$$\begin{aligned}\frac{1}{m_c}G^0_C(0) &= \frac{1}{2\beta}\sum_{nk}[G_1(i\omega_n,k)+g_2(i\omega_n,k)]\frac{1}{m_c},\\ \frac{1}{m_c}G^3_C(0) &= \frac{1}{2\beta}\sum_{nk}[G_1(i\omega_n,k)-g_2(i\omega_n,k)]\frac{1}{m_c},\\ -\frac{1}{2m_f}G_f(0) &= \frac{1}{2\beta}\sum_{nk}G_f(i\omega_n,k)\frac{1}{m_f}.\end{aligned}$$

These are exactly canceled by similar terms in Λ coefficients, so that sum of the two has the form

$$\frac{\mathcal{L}_{sp+dia}}{N}=\sum_{\nu=1}^{d}\Big\{2\Gamma v_\Gamma^2(A^0_\nu+A^3_\nu-A^f_\nu)^2+\frac{v_g^2}{2g}[(A^1_\nu)^2+(A^2_\nu)^2]\Big\},$$

with the coefficients

$$2\Gamma v_\Gamma^2=\frac{1}{2\beta}\sum_{nk}G^2_{1f}(i\omega_n,k)\frac{k_\nu^2}{m_cm_f}\tag{C27}$$

$$\frac{v_g^2}{2g}=2\Gamma v_\Gamma^2-\frac{1}{2\beta}\sum_{nk}[G_1(i\omega_n,k)-g_2(i\omega_n,k)]^2v_c^2,\tag{C28}$$

again anticipating the Higgs- and the NLσM terms. Note that in absence of magnetic coupling between the spins

the f-electrons are localized $m_f \to \infty$ and consequently $v_\Gamma^2 \to 0$. Carrying out the Matsubara sum, we obtain

$$2\Gamma v_\Gamma^2 = \frac{1}{m_c m_f} \int_{\text{B.Z.}} \frac{\mathrm{d}^2 k}{(2\pi)^2} \frac{V^2 k_\nu^2}{\left[(\epsilon_k^c - \epsilon_k^f)^2 + 4V^2\right]^{3/2}}, \tag{C29}$$

$$\frac{v_g^2}{2g} = 2\Gamma v_\Gamma^2 - \frac{1}{2m_c^2} \int_{\text{B.Z.}} \frac{\mathrm{d}^2 k}{(2\pi)^2} \left\{ f'(\epsilon_k^c) - \frac{V^2}{\left[(\epsilon_k^c - \epsilon_k^f)^2 + 4V^2\right]^{3/2}} - \frac{4}{(\epsilon_k^c - \epsilon_k^f) + \sqrt{(\epsilon_k^c - \epsilon_k^f)^2 + 4V^2}} \right.$$
$$\left. - \frac{2}{\sqrt{(\epsilon_k^c - \epsilon_k^f)^2 + 4V^2}} + \frac{2f(\epsilon_k^c)(\epsilon_k^c - \epsilon_k^f)}{V^2} \right\} k_\nu^2, \tag{C30}$$

here we have again set the Fermi functions to $f(E^h) = 1$ and $f(E^l) = 0$, because we have a Kondo insulator at $T \ll T_K$. In this limit the momentum integrals can be obtained analytically for the continuum model in $d = 2$ spatial dimensions:

$$2\Gamma v_\Gamma^2 = \frac{\pi \nu^2 V}{2 m_c m_f} \left[\sqrt{1+\eta^2} + \eta\right] \tag{C31}$$

$$\frac{v_g^2}{2g} = 2\left(1 + \frac{m_f}{m_c}\right) \Gamma v_\Gamma^2 - \frac{1}{2\pi} \left\{ \eta - \frac{4}{3}\left[(\eta^2+1)^{3/2} + \eta^3\right] + 2\sqrt{\eta^2+1} + 2\eta^2 \left[\eta + \sqrt{\eta^2+1}\right] \right\} + \frac{\mu}{4\pi} + \frac{\mu^3}{12\pi V^2} \tag{C32}$$

To lowest order in T_K/D and $r_m = m_c/m_f$ these coefficients simplify to

$$2\Gamma v_\Gamma^2 \approx \frac{\pi}{2} r_m D, \tag{C33}$$

$$\frac{v_g^2}{2g} \approx \frac{D}{\pi}. \tag{C34}$$

3. Alternative representation

Using the parametrization (54) we have

$$(A_\nu^1)^2 + (A_\nu^2)^2 = (\partial_\nu \theta)^2 + (\partial_\nu \phi)^2 \sin^2\theta = (\partial_\nu \vec{n})^2 \tag{C35}$$

where we have used the Hopf map $\vec{n} = z^\dagger \vec{\sigma} z$. Moreover,

$$A_\nu^3 = \partial_\nu \varphi + \partial_\nu \phi \cos\theta = -i z^\dagger \partial_\nu z \tag{C36}$$

Note that the 'magnetic field' associated with this vector potential is equal to the topological charge

$$B_\mu = \epsilon_{\mu\lambda\nu} \partial_\lambda A_\nu^3 = \epsilon_{\mu\lambda\nu} \vec{n} \cdot (\partial_\lambda \vec{n} \times \partial_\nu \vec{n}). \tag{C37}$$

For the example, in two dimensions, B_z is the density of the skyrmions.

The coefficients computed in the previous section can be used to write the Lagrangian in the following form

$$\mathcal{L} = \frac{1}{2g}\left[(\partial_\tau \vec{n})^2 + v_g^2 \sum_{a=1}^{d} (\partial_a \vec{n})^2\right] \tag{C38}$$
$$+ \frac{\Gamma}{2}\left[(\tfrac{1}{2}\Omega_\tau^z - (A_\tau^{ext} - A_\tau^f))^2 + v_\Gamma^2 \sum_{a=1}^{d} (\tfrac{1}{2}\Omega_a^z - (A_a^{ext} - A_a^f))^2\right],$$

where we have restored $A_\mu^3 = \frac{1}{2}\Omega_\mu^z$ and the parameters are given by

$$\frac{1}{2g} \approx \nu \mathcal{Z} \tag{C39}$$

$$2\Gamma \approx \frac{\nu}{2} \tag{C40}$$

$$v_g^2 \approx \frac{D}{\pi \nu \mathcal{Z}} \tag{C41}$$

$$v_\Gamma^2 \approx \frac{\pi r_m D}{2\nu}. \tag{C42}$$

where $\mathcal{Z} = \left[1 + t_K(1 + r_m/t_K)^2\right]$ was defined before. Using $D = \tilde{q}_f/\nu$, $\nu \approx \rho = m_c/2\pi$ and $\tilde{q}_f = k_F^2/4\pi$ we find the expressions reported in Eq. (66).

[1] P. Nozières and A. Blandin, J. Phys. France **41**, 193 (1980).

[2] N. Andrei and C. Destri, Phys. Rev. Lett. **52**, 364 (1984).

[3] A. M. Tsvelick and P. B. Wiegmann, Zeit. Phys B , 201 (1984).
[4] I. Affleck, A. W. W. Ludwig, H.-B. Pang, and D. L. Cox, Phys. Rev. B **45**, 7918 (1992).
[5] I. Affleck and A. W. W. Ludwig, Phys. Rev. B **48**, 7297 (1993).
[6] V. J. Emery and S. Kivelson, Phys. Rev. B **46**, 10812 (1992).
[7] A. M. Sengupta and A. Georges, Phys. Rev. B **49**, 10020 (1994).
[8] H. B. Pang and D. L. Cox, Phys. Rev. B **44**, 9454 (1991).
[9] P. Coleman, L. B. Ioffe, and A. M. Tsvelik, Phys. Rev. B **52**, 6611 (1995).
[10] D. L. Cox and M. Jarrell, Journal of Physics: Condensed Matter **8**, 9825 (1996).
[11] P. Chandra, P. Coleman, and R. Flint, Nature **493**, 621 (2013).
[12] T. Onimaru and H. Kusunose, J. Phys. Soc. Jpn. **85**, 082002 (2019).
[13] A. Wörl, T. Onimaru, Y. Tokiwa, Y. Yamane, K. T. Matsumoto, T. Takabatake, and P. Gegenwart, Phys. Rev. B **99**, 081117(R) (2019).
[14] Y. Komijani, A. Toth, P. Chandra, and P. Coleman, arXiv:1811.11115 (2018).
[15] M. Jarrell, H. Pang, D. L. Cox, and K. H. Luk, Phys. Rev. Lett. **77**, 1612 (1996).
[16] M. Jarrell, H. B. Pang, and D. L. Cox, Physical Review Letters **78**, 1996 (1997).
[17] A. M. Tsvelik and C. I. Ventura, Phys. Rev. B **61**, 15538 (2000).
[18] S. Hoshino, J. Otsuki, and Y. Kuramoto, Phys. Rev. Lett. **107**, 247202 (2011).
[19] S. Hoshino, J. Otsuki, and Y. Kuramoto, Journal of the Physical Society of Japan **82**, 044707 (2013).
[20] S. Hoshino and Y. Kuramoto, Journal of Physics: Conference Series **592**, 012098 (2015).
[21] G. Zhang, J. S. Van Dyke, and R. Flint, Phys. Rev. B **98**, 235143 (2018).
[22] J. S. Van Dyke, G. Zhang, and R. Flint, Phys. Rev. B **100**, 205122 (2019).
[23] M. Oshikawa, Phys. Rev. Lett. **84**, 3370 (2000).
[24] R. M. Martin, Phys. Rev. Lett. **48**, 362 (1982).
[25] N. Read and D. Newns, J. Phys. C **16**, 3274 (1983).
[26] P. Coleman, *Introduction to Many-Body Physics* (Cambridge University Press, 2015).
[27] A. C. Hewson, *The Kondo Problem to Heavy Fermions*, Cambridge Studies in Magnetism (Cambridge University Press, 1993).
[28] B. Coqblin and J. R. Schrieffer, Phys. Rev. **185**, 847 (1969).
[29] A. Altland and B. D. Simons, "Broken symmetry and collective phenomena," in *Condensed Matter Field Theory* (Cambridge University Press, 2010) p. 242359, 2nd ed.
[30] J. B. Marston and I. Affleck, Phys. Rev. B **39**, 11538 (1989).
[31] A. M. Polyakov, *Gauge Fields and Strings* (CRC Press, 1987).
[32] P. Coleman, J. B. Marston, and A. J. Schofield, Phys. Rev. B **72**, 245111 (2005).
[33] J. Zinn-Justin, *Quantum Field Theory and Critical Phenomena* (Oxford Scholarship Online, 2002).
[34] S. Sachdev, *Quantum Phase Transitions*, 2nd ed. (Cambridge University Press, 2011).
[35] N. Andrei and E. Orignac, Phys. Rev. B **62**, R3596 (2000).
[36] T. Schauerte, D. L. Cox, R. M. Noack, P. G. J. van Dongen, and C. D. Batista, Phys. Rev. Lett. **94**, 147201 (2005).
[37] A. A. Belavin and A. M. Polyakov, JETP Lett. , 245 (1975).
[38] Y. Komijani and P. Coleman, Phys. Rev. Lett. **120**, 157206 (2018).
[39] Y. Komijani and P. Coleman, ArXiv: 1810.08148 (2018).
[40] N. Read and S. Sachdev, Phys. Rev. B **42**, 4568 (1990).
[41] T. Senthil, A. Vishwanath, L. Balents, S. Sachdev, and M. P. A. Fisher, Science **303**, 1490 (2004).
[42] T. Senthil, S. Sachdev, and M. Vojta, Phys. Rev. Lett. **90**, 216403 (2003).